

Metadata of the chapter that will be visualized online

Chapter Title	Infrared, Raman, and Fluorescence Spectroscopies: Methodologies and Applications	
Copyright Year	2013	
Copyright Holder	Springer Science+Business Media New York	
Corresponding Author	Family Name	González
	Particle	
	Given Name	Diego L. García
	Suffix	
	Organization	Instituto de la Grasa (CSIC)
	Address	Avda. Padre García Tejero 4, 41012, Seville, Spain
	Email	dluisg@cica.es
Author	Family Name	Baeten
	Particle	
	Given Name	Vincent
	Suffix	
	Organization	Walloon Agricultural Research Centre
	Address	Chaussée de Namur 24, 5030, Gembloux, Belgium
Author	Family Name	Pierna
	Particle	
	Given Name	Juan A. Fernández
	Suffix	
	Organization	Walloon Agricultural Research Centre
	Address	Chaussée de Namur 24, 5030, Gembloux, Belgium
Author	Family Name	Tena
	Particle	
	Given Name	Noelia
	Suffix	
	Organization	Instituto de la Grasa (CSIC)
	Address	Avda. Padre García Tejero 4, 41012, Seville, Spain
Abstract	Spectroscopic techniques have emerged in food analysis as rapid and very useful tools for determining a great variety of chemical parameters. They provide elegant, fast, and easy-to-use solutions to tackle analytical challenges as well as a cost reduction. They offer the possibility to control a high number of parameters and properties simultaneously at the different steps of the food	

and feed chains and can be applied online. Huge instrumental and computer improvements have contributed to the development of near-infrared (NIR), mid-infrared (MIR), Raman, and fluorescence spectroscopies.

In the field of fats and oils, spectroscopic techniques can be applied to determine unsaturation degree, oxidation state, moisture, *trans* double bonds, free fatty acids, and the presence of impurities or other edible oils, among many others. Such applications require more research to improve calibration performance without losing the advantageous feature of being rapid methods. It delivers methodologies that can be eligible as standard methods to alleviate complex olive oil analysis.

In this chapter, the theory and instrumentation currently used in infrared, Raman, and fluorescence spectroscopy for the analysis of oils is presented, as well as a complete description of data acquisition, interpretation of oil spectra, assignment of the most noteworthy bands, correlation between absorption intensities, and chemical indices and chemometric data treatment for quantitative and qualitative analyses. A review of the potential offered by the spectroscopic techniques is also included.

Chapter 10 1
Infrared, Raman, and Fluorescence 2
Spectroscopies: Methodologies 3
and Applications 4

Diego L. García González, Vincent Baeten, Juan A. Fernández Pierna, 5
and Noelia Tena 6

Contents

10.1	Introduction.....	000
10.2	Theory.....	000
10.2.1	Infrared Spectroscopy.....	000
10.2.2	Raman Spectroscopy.....	000
10.2.3	Fluorescence Spectroscopy.....	000
10.2.4	Band Position and Intensity.....	000
10.3	Instrumentation.....	000
10.3.1	Near-Infrared (NIR) Spectroscopy.....	000
10.3.2	Mid-Infrared Spectroscopy.....	000
10.3.3	Raman Spectroscopy.....	000
10.3.4	Fluorescence Spectroscopy.....	000
10.3.5	Online Analysis.....	000
10.4	Data Acquisition.....	000
10.5	Interpretation of Oil Spectra.....	000
10.5.1	Near-Infrared Spectra.....	000
10.5.2	Mid-Infrared Spectra.....	000
10.5.3	Raman Spectra.....	000
10.5.4	Fluorescence Spectra.....	000
10.6	Data Treatment.....	000
10.6.1	Pretreatment of Data.....	000
10.6.2	Mathematical Model Construction.....	000
10.6.3	Validation Procedures.....	000
10.7	Potential of Infrared and Raman Spectroscopy.....	000
10.7.1	Determination of Unsaturation Degree: Iodine Value.....	000
10.7.2	Determination of <i>Trans</i> and <i>Cis</i> Content.....	000

D.L.G. González (✉) • N. Tena
 Instituto de la Grasa (CSIC), Avda. Padre García Tejero 4, 41012 Seville, Spain
 e-mail: dluisg@cica.es

V. Baeten • J.A.F. Pierna
 Walloon Agricultural Research Centre, Chaussée de Namur 24, 5030 Gembloux, Belgium

10.7.3	Determination of Saponification Number, Solid Fat Index, and Free Fatty Acids	000
10.7.4	Monitoring the Oxidative Process, Measuring the Peroxide and Anisidine Values.....	000
10.8	Potential of Fluorescence Spectroscopy	000
10.9	Conclusions.....	000
	References.....	000

7 **Abbreviations**

8	ANN	Artificial neural network
9	ATR	Attenuated total reflection
10	CCD	Coupled charge device
11	CV	Coefficient of variation
12	EEFS	Excitation-emission fluorescence spectroscopy
13	FF	Front face
14	FT	Fourier transform
15	IRE	Internal reflection element
16	MIR	Mid-infrared
17	MLR	Multiple linear regression
18	MSE	Multiple standard error
19	NIR	Near-infrared
20	NMR	Nuclear magnetic resonance
21	OPL	Optical path length
22	PCA	Principal component analysis
23	PLSR	Partial least-squares regression
24	PLS	Partial least squares
25	PLSDA	Partial least-squares discriminant analysis
26	RA	Right angle
27	RHM	Resampling by half-means
28	SD	Standard deviation
29	SFS	Synchronous fluorescence spectroscopy
30	SHV	Smallest half-volume
31	SLDA	Stepwise linear discriminant analysis
32	SMLR	Stepwise multiple linear regression
33	SVM	Support vector machine

34 **10.1 Introduction**

35 Spectroscopic techniques have emerged in food analysis as rapid and very useful
 36 tools for determining a great variety of chemical parameters. They provide elegant
 37 solutions to face analytical challenges. In spite of the intense research on spectro-
 38 scopic techniques during the twentieth century, the application of such techniques

has been delayed due to the spread of chromatography, which allows an easy quantitative interpretation of results, and the lack of suitable sample presentation techniques, chemometric tools to calibrate and standardize instruments, intuitive chemometric tools, and standardized protocols for spectroscopy. However, the necessity of reducing the analytical time and cost, the high number of parameters and properties to be simultaneously controlled at the different steps of the food and feed chains, and the increasing demand for online techniques, as well as the relative limit of traditional techniques to solve some analytical questions faced by the control laboratories and industries, have rekindled interest in spectroscopy techniques. Furthermore, instrumental improvements such as the introduction of interferometry methodology and the diode array detector, the availability of new sample-handling accessories, the miniaturization of instruments, the computer facilities, and the existence of software specially designed to extract and to use the information contained in spectra have contributed to the development of near-infrared (NIR), mid-infrared (MIR), Raman, and fluorescence spectroscopies. These significant improvements have led to less sophisticated and expensive instruments that could be used on a regular basis at any laboratory without requiring any special skills or training.

[AU1]

In the field of fats and oils quantitative applications are relatively recent compared to qualitative methodologies. These quantitative procedures have benefited from new ways of calibration (e.g., signal-transduction calibration), adapted accessories for sample presentation (e.g., ATR, IR cards, and mesh cells), and adopted new procedures of spectra interpretation (e.g., 2D correlation spectroscopy). The great variety of optical materials and sampling approaches makes the spectroscopic techniques much more versatile than other methodologies, which explains the growing interest in developing quantitative applications. Although there are only few standard methodologies for olive oil analysis based on spectroscopy (e.g., determination of dienes and trienes by ultraviolet spectroscopy, COI/T.20/Doc. No 19/Rev. 2), a spectroscopic technique such as Fourier transform infrared spectroscopy (FTIR) can be applied to determine the unsaturation degree, oxidation state, moisture content, *trans* double bonds, free fatty acids, and the presence of impurities or other edible oils, among many others. Such applications require more research to improve calibration performance without losing the advantageous feature of being rapid methods. Such research might deliver methodologies that could be eligible as standard methods in the future to alleviate complex olive oil analysis.

[AU3]

[AU4]

In this chapter, the second and third sections briefly present the theory and instrumentation currently used in IR, Raman, and fluorescence spectroscopies for the analysis of oils. The fourth section describes data acquisition, and the fifth section is dedicated to interpretation of oil spectra. The assignment of the most noteworthy bands and the correlation between absorption (or scattering) intensities and chemical indices are discussed. Part of this chapter (the sixth section) is devoted to the data treatment of IR and Raman spectra. In this section, a mathematical model construction in quantitative and qualitative analyses is presented. Finally, the results obtained in the determination of chemical values and indices are surveyed in the seventh section.

85 **10.2 Theory**

86 The importance of spectroscopy becomes apparent from a reading of the classic text
87 published by Herzberg (1945). However, it was not until recently that dramatic progress
88 was made with the advent of IR lasers (e.g., IR circular dichroism) and interferometric
89 methods, the introduction of high-power and pulsed lasers (e.g., hyper-Raman and
90 coherent anti-Stokes-Raman scattering), or attenuated total reflection (ATR) spectroscopy,
91 among others. Thus, spectroscopy is not a static field; it is a quite dynamic and
92 innovative area. Regarding vibrational spectroscopy, the basic theory has been described
93 in ten or so classic books on spectroscopy, some of which are compilations of data while
94 others are comprehensive texts (Wilson et al. 1955; Williams and Norris 2001; Li-Chan
95 et al. 2010a, b). Most practical books usually emphasize the correlation between
96 molecular structural features and frequencies (Socrates 1994), while textbooks are
97 devoted to explaining the theory of vibrational spectroscopy (Williams and Norris 2001;
98 Diem 1993). Concerning fluorescence spectroscopy, modern manuals explaining the
99 fundamentals and applications illustrate the increasing interest in this technique for
100 developing applications beyond basic research (Valeur 2002).

101 The following section will briefly describe those theoretical aspects of IR, Raman,
102 and fluorescence spectroscopies that are basic for understanding spectroscopic
103 analyses.

104 **10.2.1 Infrared Spectroscopy**

105 Infrared spectroscopy is a technique in which the interaction of electromagnetic
106 radiation with a sample is studied to obtain both qualitative and quantitative chemical
107 information. The IR region lies between the red end of the visible spectrum and the
108 microwave region. It comprises wavelengths (λ) between 800 and 2.5×10^5 nm. The IR
109 region of the electromagnetic spectrum is subdivided into NIR ($\lambda=0.8\text{--}2.5$ μm), MIR
110 ($\lambda=2.5\text{--}25$ μm), and far-IR ($\lambda=50\text{--}1,000$ μm). These distinctions are based on the
111 nature of the absorptions giving rise to the corresponding spectra, as well as differences
112 in instrumental design and experimental approach. All are parts of vibrational spectroscopy
113 and arise from transitions between vibrational energy levels (Banwell 1994).

114 The simplest approach to explaining the phenomenon occurring in vibrational
115 spectroscopy is to consider the bond between two atoms of masses m_1 and m_2 as
116 behaving as a tiny spring of “strength,” or force constant k ($\text{N}\cdot\text{m}^{-1}$). The system will
117 vibrate at some natural resonance frequency ν (s^{-1}) given by Hooke’s law:

$$\nu = \frac{1}{2\pi} \sqrt{\frac{\kappa}{\mu}}$$

118

119 where μ is the “reduced mass” ($[m_1 m_2 / (m_1 + m_2)]$). This approach is used to explain
120 the observed difference in absorption frequencies between different functional
121 groups on the basis of different force constants or reduced masses.

[AU5]

However, the quantum theory needs to be considered here. The energy E (J) of a photon of wavelength λ (m) is

$$E = h\nu = h \frac{c}{\lambda}$$

In this equation h (J.s) is Planck's constant and c (m.s⁻¹) is the velocity of light.

Hooke's law for a simple harmonic oscillator model predicts a potential energy curve as a parabolic function of the interatomic distance. The potential energy is minimized at the equilibrium nuclear distance. Increasing interatomic distance leads to increased potential energy in a continuous manner. In a quantum mechanical approach (corpuscular theory), however, only certain energy levels are permitted. These energy levels are given by

$$E(n) = \left(n + \frac{1}{2} \right) h\nu$$

where $n=0,1,2,\dots$ is the vibrational quantum number. Transition between energy levels can only occur in discrete steps when sufficient energy E is provided, i.e.,

$$\Delta E = h\nu$$

Transitions occur when $n \geq \pm 1$. The molecule will absorb the energy of the photon if it precisely matches the energy that is required for the transition between energy levels and when there is a change in the dipole moment associated with the vibration. The transitions in which $n = \pm 1$ are called fundamental vibrations and they are observed in MIR spectroscopy. The energy required to stimulate these transitions occurs at wavelengths between 2,500 and 25,000 nm (4,000–400 cm⁻¹).

In fact, vibrating bonds are anharmonic oscillators. When the interatomic distance becomes very small, atomic repulsion causes the potential energy to rise dramatically. As the interatomic distance increases, the bond will initially stretch and eventually break. This anharmonic behavior can be incorporated into the Schrödinger equation and leads to a new expression for permitted energy levels:

$$E(n) = \left(n + \frac{1}{2} \right) h\nu - \left(n + \frac{1}{2} \right)^2 x_e h\nu$$

where x_e is a small and positive anharmonicity constant.

As a result of anharmonicity, energy levels become closer as n increases and transitions of the type $n = \pm 2$, $n = \pm 3$, or overtones are allowed. In addition, a combination band is produced when the photon excites simultaneously the vibration of two or more interatomic bonds that are sufficiently close to influence their respective vibrations. Combinations and overtones are seen at higher energy (lower wavelength) and occur in the NIR region (800–2,500 nm; 10,000–4,000 cm⁻¹). These bands have lower intensity than fundamental bands. Figure 10.1 illustrates the anharmonic oscillator and the different associated energetic transitions (Barrow 1973; Williams and Norris 2001; Skoog et al. 1992).

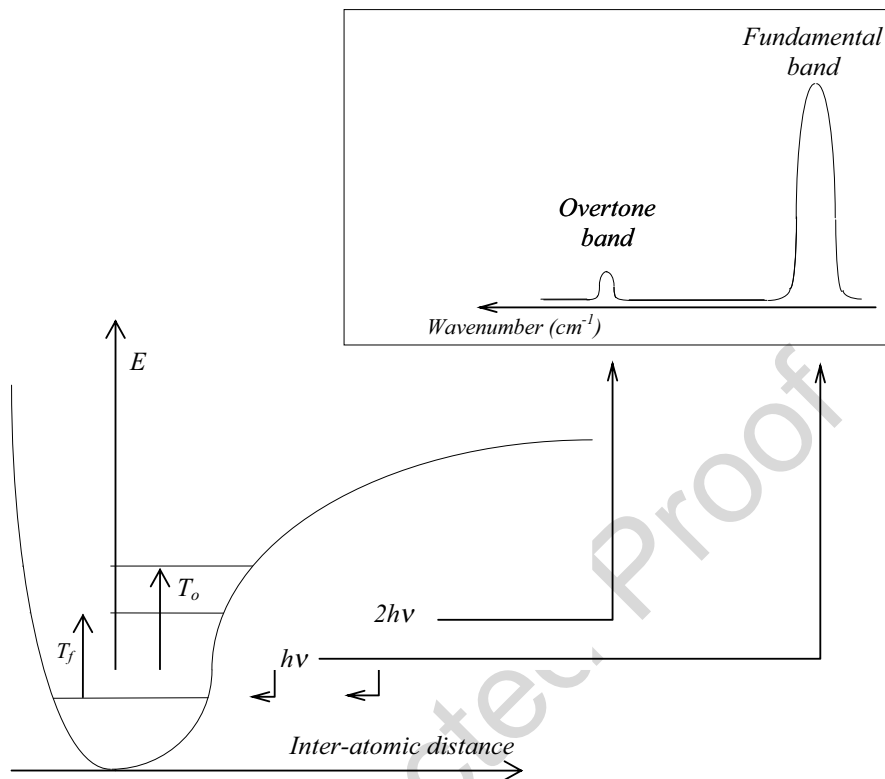


Fig. 10.1 Anharmonic oscillator and associated energetic transitions. Legend: E potential energy, T_f fundamental transition, T_o overtone transition

158 **10.2.2 Raman Spectroscopy**

159 Raman spectroscopy involves a scattering process. When the electric field E interacts
 160 with a molecule, it exerts the same force on all electrons in the molecule and tends to
 161 displace them from their original position around the positively charged nuclei. The
 162 displacements result in an induced dipole moment π in the molecule that is proportional
 163 to the electric field:

[AU6]

164
$$\pi = \alpha E,$$

165 where α is the electric polarizability. Since π depends on α as well as E , the properties
 166 of the molecule can change π . In this context, α varies with time as a consequence of
 167 the vibrations of the molecule since the ease with which electrons may be displaced
 168 by the electric field depends on how tightly they are bound to the nuclei, which in
 169 turn depends on the interatomic distance.

When the electric field interacts with a vibrating molecule, the induced dipole moment has three components contributing to its time dependence. The first is a component vibrating with the frequency of the incident light. According to classical electromagnetic theory, an oscillating dipole radiates energy in the form of scattered light. Thus, the first component, light of the incident frequency (ν_{Ray}), will be scattered. This is the phenomenon of Rayleigh scattering. The second component is the one vibrating at a frequency that is the sum of the frequencies of the incident light and the molecular vibration. The scattered light arising from this second component is known as anti-Stokes Raman scattering ($\nu_{R(aSt)}$). The third component is the vibration at a frequency given by that of the incident light minus the molecular vibrations. This is called Stokes scattering ($\nu_{R(S)}$) (Grasselli and Bulkin 1991; Diem 1993; Schrader 1996).

Figure 10.2 shows an energy diagram of the Raman scattering effect and illustrates a schematic and simplified Raman spectrum. To simplify the presentation, only two electronic states (the ground and the first excited) and three vibrational states of each of them are shown. The intensity of the anti-Stokes Raman scattering bands of frequency $<_{R(aSt)}$ is lower than the intensity of Stokes Raman scattering bands of frequency $<_{R(S)}$ in view of the difference in population of the ground excited electronic states in a set of molecules at room temperature (Baranska et al. 1987). The Raman spectra studied and presented later on in this chapter concern only Raman Stokes scattering bands.

10.2.3 Fluorescence Spectroscopy

Fluorescence spectroscopy is a type of electromagnetic spectroscopy in which the fluorophore groups included in the samples are excited using a beam of light. Usually ultraviolet light is used and the emission of light of a lower energy is observed; typically, but not necessarily, the emission is in the visible range of the electromagnetic spectrum. In particular, conventional fluorescence spectroscopy provides an emission spectrum for a fixed excitation wavelength or an excitation spectrum for a fixed emission wavelength. The emission spectra are obtained by recording the signal of an emission monochromator at different wavelengths (λ_{em}) for a constant excitation wavelength (λ_{ex}), usually at a wavelength of high absorption. On the other hand, the excitation spectra are obtained by recording the signal from the excitation monochromator at different wavelengths (λ_{ex}), maintaining a constant emission wavelength (λ_{em}). The spectra provide information for both qualitative and quantitative analyses about fluorophore groups present in the sample. However, the applications of fluorescence spectroscopy in the characterization of edible oils are scarce because the fluorescence characteristics of fluorophores are affected by the matrix. Although molecular fluorescence spectroscopy is a highly sensitive technique, a severe overlap of excitation and emission makes the spectra difficult to interpret (Patra and Mishra 2002). The fluorescence spectra can also be affected by the attenuation of the absorption intensity due to the absorption of the excitation wavelength (primary inner effect) and the

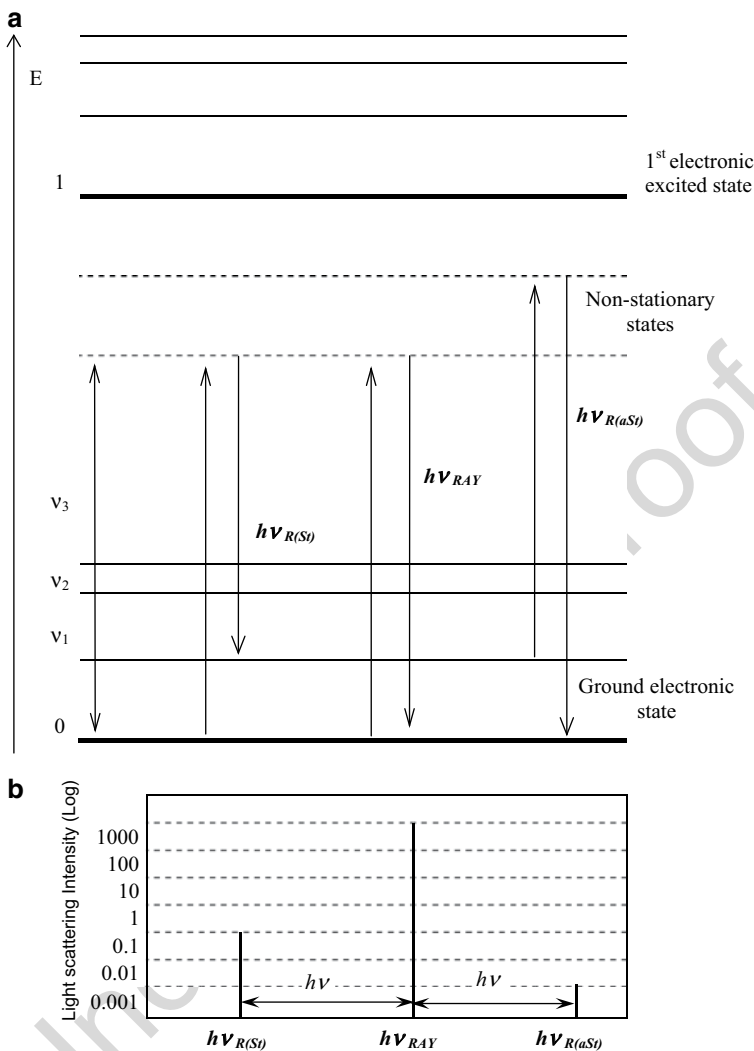


Fig. 10.2 (a) Raman scattering effect occurring during illumination of sample with monochromatic light. (b) Part of resulting Raman spectrum. Legend: E electronic state, I light-scattering intensity (log scale), ν_{RAY} frequency of Rayleigh line, $\nu_{R(aSI)}$ frequency of anti-Stokes Raman line, $\nu_{R(SI)}$ frequency of Stokes Raman line (Adapted from Baranska et al. 1987)

211 emission wavelength (secondary inner effect) (Sikorska et al. 2004). These phenomena
 212 are more evident when working with right angle (RA) instruments (Lakowicz 1999). In
 213 RA instruments, the collection of the fluorescence beam is collected at a right angle to
 214 the incident light. In other words, the emission is measured at 90° in relation to the
 215 excitation beam. In contrast, in modern front face (FF) instruments, the fluorescence
 216 beam is collected at an approximately $22\text{--}30^\circ$ angle relative to the incident beam. This
 217 geometry minimizes the inner filter effects compared to RA instruments.

10.2.4 Band Position and Intensity

218

In vibrational spectroscopy, the probability of excitation for a particular vibration is determined by the so-called selection rules, which can be derived from the application of group theory to atomic vibrations in the molecules belonging to different classes of symmetry. Some factors tend to modify the band positions (i.e., vibration frequencies). The most important factors are the interatomic distances, the spatial arrangement groups, the Fermi resonance, the physical state of the sample, the polarity of the environment, the formation of hydrogen bonds, and the inductive, mesomeric, and field effects of neighboring groups. In this way, the difference in the force constant, for example, explain that the stretching frequency of double bonds is higher than those of single bonds (Baranska et al. 1987; Grasseli and Bulkin 1991; Diem 1993).

Infrared and Raman spectroscopy involve vibrational energy levels of the sample molecules that are related primarily to stretching or bending deformations of the molecular bonds. However, two main differences should be underlined between IR and Raman spectra. First, IR peaks tend to be broad and it is difficult to find a peak that is completely free of the influence of adjacent peaks or external parameters. On the other hand, a Raman spectrum tends to be composed of a series of isolated bands, and water and CO₂ have weak Raman scattering properties and, consequently, produce less interference in Raman scattering spectroscopy. Another difference is that polar groups (such as C=O and O-H) have strong IR absorption bands, whereas nonpolar groups (such as C=C and C-C) show intense Raman scattering bands. These two branches of vibrational spectroscopy in fact yield complementary information about molecular vibration, each one contributing to a spectral fingerprint of the molecules (Li-Chan 1994).

From a chemical point of view, Raman scattering arises from the change in polarizability or shape of the electron distribution in the molecule as it vibrates; in contrast, IR absorption requires a change in the intrinsic dipole moment with the molecular vibration (Grasseli and Bulkin 1991). More accurately, the Raman band intensity is proportional to the expression

$$(\partial\alpha/\partial Q)^2,$$

where α is the polarizability and Q the normal coordinate of the group of atoms of interest. The IR band intensity is proportional to the expression

$$(\partial\pi/\partial Q)^2,$$

where π is the induced dipole moment of the molecule. Thus, it might be expected that the same molecule may give IR and Raman bands with differing intensities and band shapes (Baranska et al. 1987).

Concerning fluorescence spectroscopy, to study the band position and intensity it is necessary to consider the following issues:

- 257 1. The excitation wavelength used to obtain the emissions spectra should be
258 strongly absorbed by the fluorescent compounds; therefore it is recommended to
259 obtain the full absorption spectrum of the sample and then select the excitation
260 wavelength more appropriate based on the maximum absorption intensities. It is [AU8]
261 important to use an excitation wavelength that is strongly absorbed because the
262 emission fluorescence intensity is proportional to the absorption intensity.
- 263 2. Not all of the emission spectrum obtained with the selected excitation wave-
264 length corresponds to the fluorescent compounds present in the sample.
265 According to Stokes's law of fluorescence states, the wavelength of fluorescence
266 radiation is greater than the exciting radiation. Consequently, the emission wave-
267 lengths should be at least five or ten units larger than the excitation wavelength.
268 For example, for an excitation wavelength (λ_{ex}) at 350 nm, the bands that appear
269 in the emission spectrum at wavelengths below 360 nm do not correspond to
270 fluorescent compounds.
- 271 3. Other additional considerations that could lead to error are associated with over-
272 tones. Thus, it is important to note that the overtone area is located at twice the
273 wavelength of excitation in the emission spectrum. In the interpretation of the
274 spectra it is also convenient to omit the region of the spectrum that is located too
275 far from the excitation wavelength (Fig. 10.3).
- 276 4. Primary and secondary inner filter effects are other considerations that should be
277 taken into account in the traditional RA techniques (Lakowicz 1999). The inner [AU9]
278 filter effects imply the attenuation of the emission intensity due to the absorption
279 of the incident excitation light and emitted light (Sikorska et al. 2004). These
280 effects are avoided by working with diluted samples – in the case of oils, 1 % is
281 enough. This solution also prevents saturation in the spectrum. Nevertheless, [AU10]
282 the spectra obtained from diluted samples are not always comparable to those
283 obtained with original undiluted samples. This difference in the spectra is due to
284 the original environment of the samples, which dramatically changes when they
285 are diluted, and this could have a significant effect given that fluorescence prop-
286 erties are extremely sensitive to matrix changes (Strasburg and Ludescher 1995).
287 To overcome this problem and examine native samples directly, the FF technique
288 is more appropriate.

289 10.3 Instrumentation

290 Two of the main reasons for the development of new applications of spectroscopic [AU11]
291 techniques are the simplicity of the equipment and the sample presentation. Samples
292 can be examined in their gaseous, liquid, or solid states. Enormous progress has
293 been made, particularly over the two last decades, on the instrumental front (Diem
294 1993; Sharma et al. 1999; Li-Chan et al. 2010a).

295 Spectrometers can be classified according to the radiation source used, either
296 thermal or nonthermal. Thermal sources (e.g., quartz-halogen or tungsten-halogen
297 lamps) consist of a radiant filament that produces thermal radiation covering a

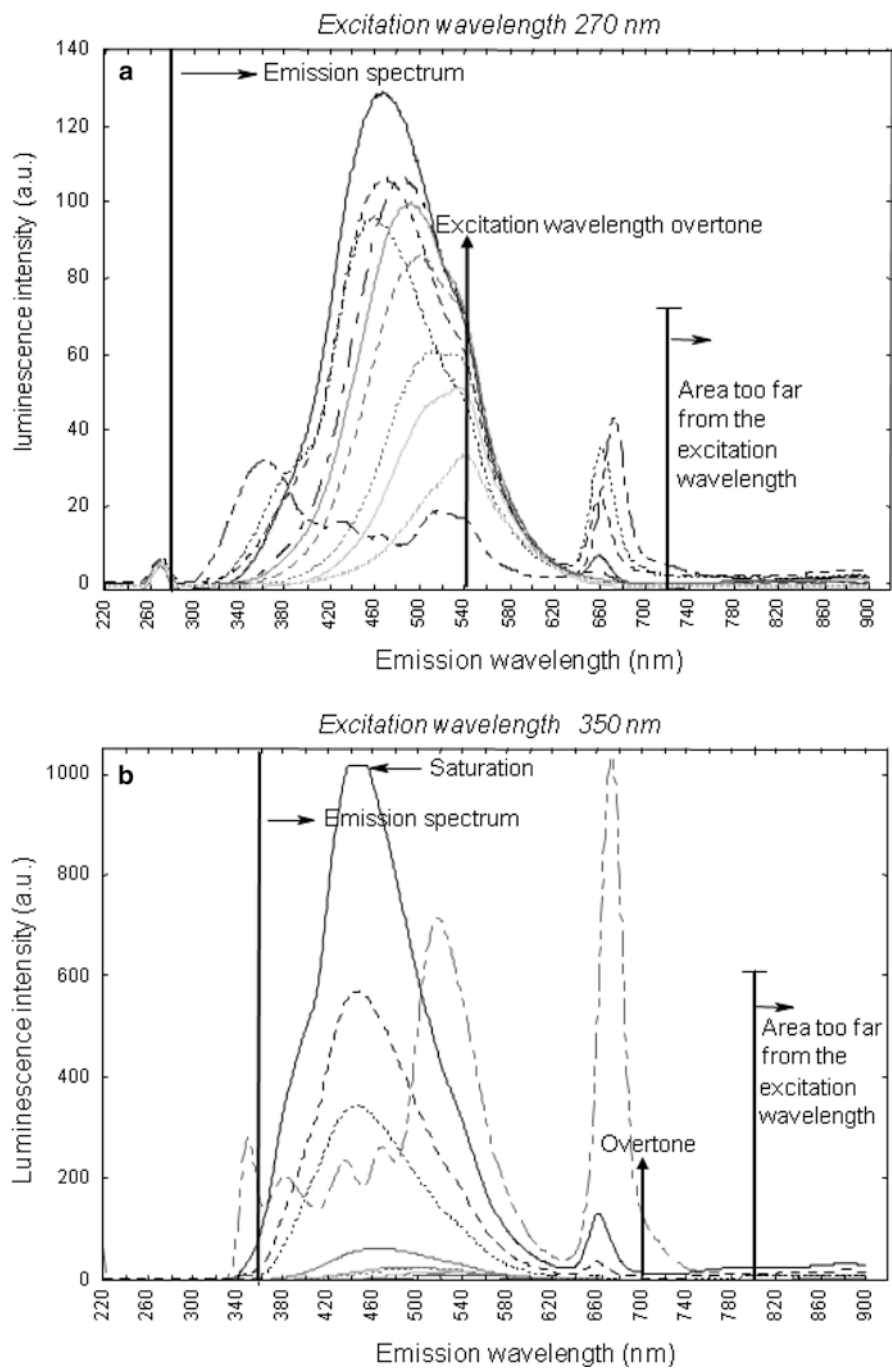


Fig. 10.3 Fluorescence emission spectra of virgin olive oils differing in oxidation degrees collected under two different excitation wavelengths: $\lambda_{exc} = 270$ nm (a) and $\lambda_{exc} = 350$ nm (b)

298 narrow or wide range of frequencies in the vibrational spectral range. Nonthermal
299 sources (e.g., light-emitting diodes, laser diodes, or lasers) emit narrower bands of
300 radiation than those emitted by thermal sources. Another classification of spectrom-
301 eters is based on the wavelength selection strategy: discrete or continuous wave-
302 length selection. Discrete wavelength instruments, using filters or light-emitting
303 diodes, make it possible to collect the absorbance at specific wavelengths and are
304 not widely used. Continuous-spectrum instruments are based on grating monochro-
305 mator, acousto-optical tunable filter, photodiode array, Fourier transform (FT) inter-
306 ferometer technologies, or microelectromechanical systems (MEMS) (Osborne
307 et al. 1993; Williams and Norris 2001; Blanco and Villaroya 2002).

308 **10.3.1 Near-Infrared (NIR) Spectroscopy**

309 NIR instruments have been widely used for nondestructive rapid analysis in several
310 important industries since the early 1970s. In the animal feed, grain, chemical, phar-
311 maceutical, and food industries, NIR spectroscopy is used in offline, online, and
312 inline modes. Several optical approaches have been used in NIR instruments,
313 including filters, holographic gratings, acousto-optically tunable filters, light-
314 emitting diodes, and the internal and external fitting of optic fibers (Scotter 1997;
315 Osborne et al. 1993, 1997; Williams and Norris 2001).

[AU12]

316 Four configurations of spectral collection exist: transmission, transflection,
317 diffuse reflection, and interactance. This has been addressed in detail by Wilson and
318 Goodfellow (1994). In oil analysis, transmission and transflection modes are tradi-
319 tionally used and correspond to specific sample-handling designs. An important
320 feature of NIR spectroscopy is that the shorter NIR wavelengths can penetrate
321 deeply into the sample; thus, it is possible to obtain spectral data from a thick sam-
322 ple (i.e., 1–5 mm). In addition, classic crystal and quartz materials are free of absor-
323 bance in the NIR region.

324 A transmission cell is used to obtain spectra of liquids and slurries. To make a
325 transmission measurement, the sample accessory is placed between the source and
326 the detector. The sample is introduced into the cell specially designed to have a
327 constant sample thickness. Transmission cells are usually constituted by two crys-
328 tal windows separated by spacers of different thicknesses, quartz cuvette of fixed
329 thickness (e.g., 1 or 5 mm), or by disposable vials of fixed width (Williams and
330 Norris 2001).

331 Transflection cells are designed for making transmittance measurements with
332 instruments that are designed only to collect reflectance spectra (i.e., instruments
333 where the source and the detectors are on the same side). A classic transflection cell
334 is an aluminum cup covered with a slide glass (crystal or quartz) and having a gold
335 plate as reflector. The energy traverses the sample once, is then reflected on the gold
336 reflector, and traverses back to the sample before reaching the detector.

[AU13]

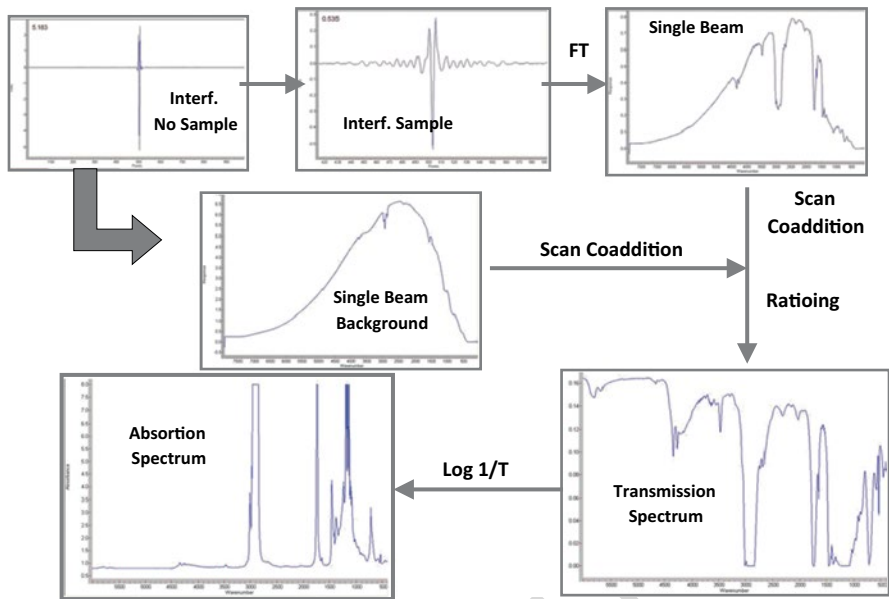


Fig. 10.4 Processing of signals in infrared spectroscopy from interferogram to absorption spectrum

10.3.2 Mid-Infrared Spectroscopy

337

Until recently, MIR spectroscopy has been of limited use for the study of food materials due to a number of drawbacks. Food samples are often opaque and highly scattering. Furthermore, they often contain high concentrations of water, which absorbs strongly in the MIR region. Food materials, therefore, are not very amenable to classic transmission techniques and sampling methods such as pellets or mulls (Wilson 1990). A second factor limiting the use of MIR spectroscopy with food samples has been that classic instrumental methods suffered from a lack of speed and from a low energy level of the sample due to the use of monochromators. However, the development of new sampling methods together with FT instruments have now made it possible to routinely analyze food samples by MIR spectroscopy (Wilson 1990; van de Voort and Ismail 1991).

338
339
340
341
342
343
344
345
346
347
348

The use of a Michelson interferometer allows much more energy to reach the sample, provides good wavelength reproducibility, and allows spectra to be collected in a very short time. Figure 10.4 shows the basic processing from the interferogram registered by a Michelson interferometer to transmission and absorption spectra. Apart from these combined advantages, it is worth noting that handling sampling is a major issue and is conditioned by the viscosity of the sample. FT MIR spectroscopy has made viable sample presentation techniques for edible oils, thus

349
350
351
352
353
354
355

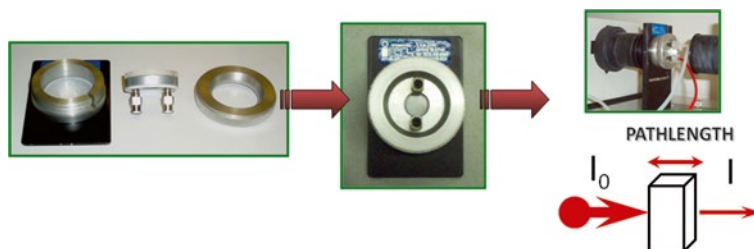


Fig. 10.5 Pictures of a typical transmission cell, demounted, assembled, and set up in **FTIR** spectrometer

356 overcoming some of their analytical problems with MIR spectroscopy. The most
 357 important MIR sample presentation techniques applicable to oil analysis are
 358 transmission liquid cell and **attenuated total reflectance (ATR) crystal**, which are
 359 described in detail by Wilson and Goodfellow (1994). Both methods require a minimum
 360 of sample preparation.

[AU14]
 [AU15]

361 10.3.2.1 Transmission Cells

362 Transmission cells allow for **FTIR** analysis in transmission mode. In this mode the
 363 sample is located in the optical path of the IR beam (I_0). Figure 10.5 shows a typical
 364 transmission cell.

365 Liquid samples, such as virgin olive oil, are normally injected into the cell to
 366 form a thin-film squeezed between two windows. There are three main types of
 367 transmission cell, all employing metal frame plates, windows to enable light to enter
 368 and leave the sample, and spacers that define the optical path length (OPL). Thus,
 369 sealed cells employ permanently bonded spacers of a fixed thickness. This first type
 370 of cell is suitable for quantitative analyses, where an invariable OPL is required. The
 371 second kind, the demountable cells, may be dismantled to facilitate cleaning and
 372 enable the use of spacers with different thicknesses and, hence, different OPLs.
 373 Finally, piston cells enable the window separation to vary continuously over a range
 374 of OPLs. In any case, the OPL variations can be controlled by adding an internal
 375 standard with a known and distinct absorption (Ismail et al. 2006).

376 Liquid cells enable reasonable quantification of solute concentrations. Practical
 377 difficulties include the maintenance of a constant (repeatable) OPL and good win-
 378 dows parallelism (to avoid wedging errors). The cell windows should be constructed
 379 from a material that is transparent to the MIR beam and, additionally, does not react
 380 with the samples. Thus, windows are commonly made of polished salt crystals
 381 (Table 10.1) that transmit IR radiation. Other materials with covalent bonds (e.g.,
 382 glass) lack this property and, in consequence, cannot be used as window material.
 383 On the other hand, given the limited energy provided by the IR source, strong absor-
 384 bance by the solvent or nontarget chemicals may dominate the absorbance spec-
 385 trum, obscuring weaker absorbance bands. Therefore, in some cases it is necessary

Table 10.1 Main characteristics of window materials used for transmission cells in FTIR spectroscopy

Window material	Working range (cm ⁻¹)	Refractive index	Advantages/disadvantages
NaCl	40,000–600	1.5	Low cost Highly hygroscopic; slightly soluble in alcohol; breaks easily
KBr	43,500–400	1.5	Low cost; good resistance Hygroscopic; soluble in alcohol and slightly in ether
KCl	33,000–400	1.5	Low cost Hygroscopic
CaF ₂	77,000–900	1.4	Insoluble in water; resists most acids and bases; high hardness (suitable for high-pressure works) Expensive
BaF ₂	66,666–800	1.5	Insoluble in water Soluble in acids and NH ₄ Cl; sensitive to mechanical shock
CsBr	42,000–250	1.7	Extended IR range Soluble in water and acids
CsI	42,000–200	1.7	Easier to handle than CsBr Hygroscopic; does not cleave; easily scratched
AgCl	25,000–434	2.0	Insoluble in water; inexpensive Darkens under UV radiation; corrosive to metals
KRS-5 (a mixed thallium bromide–thallium iodide)	20,000–285	2.37	Insoluble in acids; does not cleave Slightly water soluble
ZnSe	10,000–555	2.20	Insoluble in water and weak acids and bases Expensive; brittle; must be handled with care
ZnS	10,000–714	1.5	Insoluble in water and weak acids Expensive; slightly soluble in acids (HNO ₃ , H ₂ SO ₄ , KOH)

to use very short OPLs (below 10 μm), which are difficult to produce and measure reliably.

[AU16] One key aspect when operating with transmission cells in quantitative analysis is to know precisely the OPL to allow a correct calibration. The intensity of the IR spectral bands is determined by the OPL, which ultimately means the amount of sample between the two windows (Fig. 10.6). Then, an accurate quantitative analysis implies working under a constant and known OPL.

The procedure for determining the OPL is particularly important in demountable cells, and it should be carried out after cell assembly and prior to acquiring the spectra to make sure that no significant OPL change has resulted from the manipulation

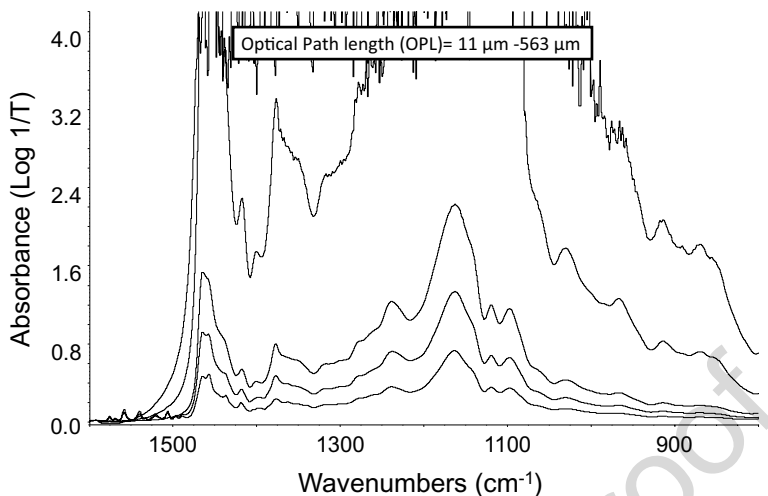


Fig. 10.6 Spectra of oils collected at different path lengths with KCl cell using spacers of several thicknesses (0.015–0.5 mm). Note: Spectra with larger OPL are off-scale

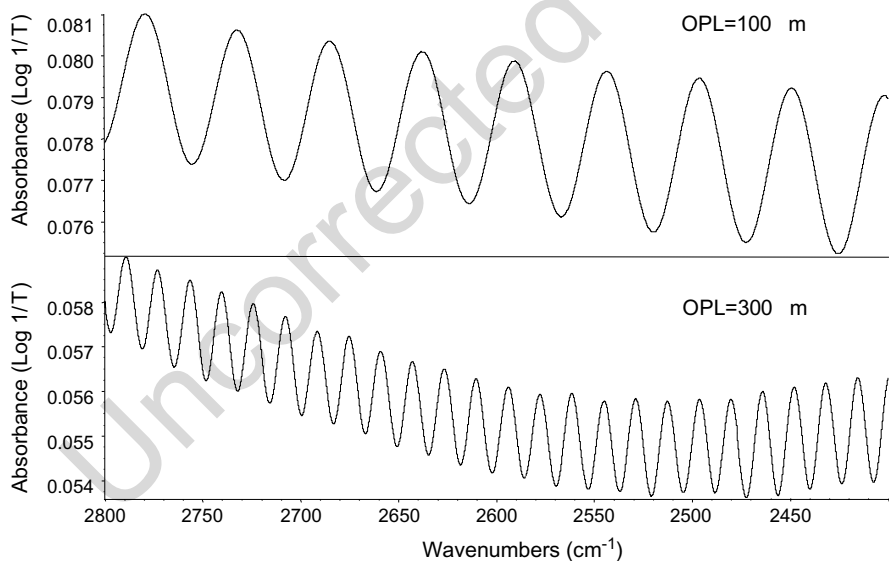


Fig. 10.7 Spectra collected from two empty transmission cells with optic path lengths (*OPL*) of 100 and 300 μm

396 of the cell. One procedure consists in acquiring a spectrum with an empty cell. The
 397 spectrum (Fig. 10.7) recorded from the empty cell is characterized by a sinusoidal line
 398 with fringes (peaks) and valleys. The OPL is calculated by counting these interference
 399 fringes between two wavenumbers and applying the following equation:

$$OPL = \frac{n}{2(v_2 + v_1)},$$
 400

where n is the number of peak-to-peak fringes, and 401
 v_1 , v_2 are the wavenumbers of the considered range. 402

Depending on the intensity of the IR band under study, the desirable OPL may 403
[AU17] lie below 100 μm . This short path length means a problem of sample handling in the 404
case of viscous liquids such as edible oils. For that reason, some new accessories 405
have been designed for this particular case to ease sample loading (in the absence of 406
bubbles) and cell cleaning. Thus, van de Voort (1994) developed a temperature- 407
controlled transmission flow cell accessory that allows for the routine use of the 408
FT-MIR technique in the quality controls of fats and oils. The instrument is composed 409
of the basic FT-MIR spectrometer, a computer that controls the instrument, a 410
temperature controller, the sample-handling accessory inlet, and control valves. 411
All components of the sample accessory are heated (usually to 80 ± 0.2 °C) so that 412
the sample can easily flow in the lines or the cell. The system includes a bypass line 413
to flush out the bulk of the previous sample, which avoids having large samples pass 414
through the cell and minimizes the cross contamination. In so doing, it is not neces- 415
sary to clean the accessory between each spectral acquisition. In summary, an oil 416
[AU18] sample is heated in the test tube block, presented at the input line, and aspired into 417
the cell using the three-way valve. 418

Another approach to facilitate sampling of viscous oils is based on the concept 419
of spectral reconstitution (SR) (van de Voort et al. 2007a). SR involves dilution with 420
a less viscous liquid. The spectra of diluted samples are then converted into good 421
facsimiles of the spectra of the neat oils, without a priori knowledge of the precise 422
dilution factor. The dilution factor is calculated from an internal IR spectral marker 423
that is added to the less viscous liquid and that does not interfere with the bands of 424
the sample. The relation of the spectral bands of the marker in the less viscous liquid 425
and the diluted samples gives information about the exact dilution factor (van de 426
Voort et al. 2008). This procedure eliminates the need for a peristaltic pump, reduces 427
sample volumes (from approximately 100 mL to approximately 5 mL), increases 428
the number of samples per hour (up to 120 samples/h), and eliminates the need for 429
solvent rinses, thereby drastically reducing disposal volumes. 430

The analysis of viscous samples with transmission cells can also be facilitated by 431
the method of signal transduction-dilution. This method has been used mainly to 432
measure acidity in mineral and edible oils (Li et al. 2009). In this procedure the 433
chemical component to be characterized (e.g., acidity) is extracted with an oil- 434
immiscible solvent (e.g., methanol) with a reagent (e.g., hydrogen cyanamide, 435
 $\text{NaHNC} \equiv \text{N}$) that reacts with the chemical component; this results in a measurable 436
band. Figure 10.8 shows this stoichiometric reaction and the spectral changes that 437
allow an accurate measurement of free fatty acid percentage. This procedure has 438
been adapted to be performed in automated (Yu et al. 2009) and portable instru- 439
ments (Li et al. 2008). The automated instrument (COAT, Thermal-Lube, Pointe- 440
Claire, QC, Canada), also used with SR, includes a demountable IR cell, pumps, 441

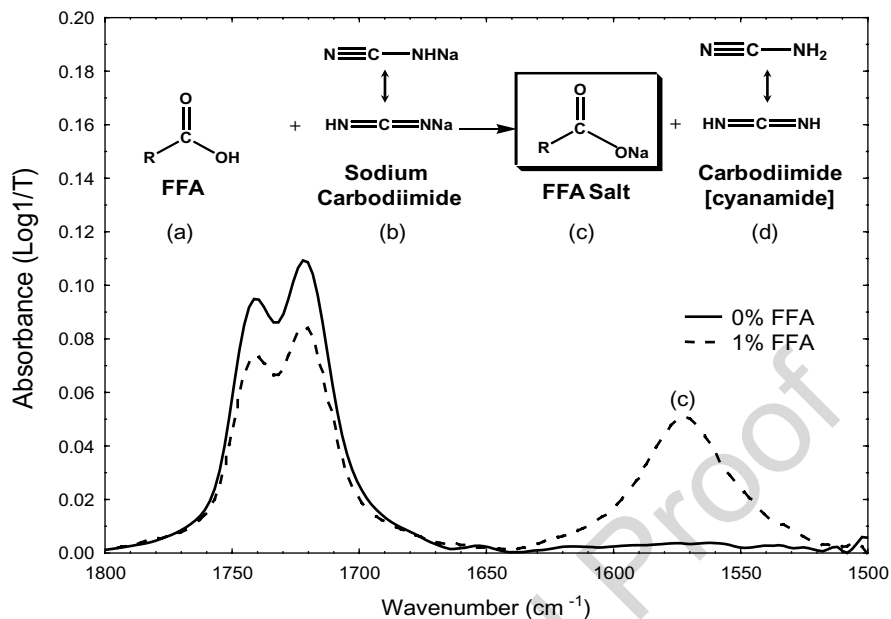


Fig. 10.8 Stoichiometric reaction associated with infrared analysis for free fatty acid (FFA) content and corresponding spectral changes taking place

442 and valves to aspirate the samples, an autosampler for automated analysis, and a
 443 specific software (UMPIRE) that automatically analyzes different chemical features
 444 and performs the mathematical operation necessary for SR (van de Voort et al.
 445 2007b). On the other hand, the portable instrument (InfraSpec VFA-IR spectrom-
 446 eter, Wilks Enterprise, South Norwalk, CT) is a low-resolution IR spectrometer with
 447 no moving parts and an electronically modulated (pulsed) source combined with a
 448 linear variable filter mounted on a detector array (VFA). This instrument has also
 449 been used coupled with an attenuated total reflection accessory in addition to trans-
 450 mission cells.

451 Although transmission cells provide a wide range of possible applications,
 452 some adaptation and new designs have been presented for a better performance in
 453 particular cases. One of these modifications involves the hyphenation of a FTIR
 454 spectrometer and another technique. Transmission flow cells are easier to hyphen-
 455 ate to other techniques in comparison with other FTIR accessories. Thus, several
 456 systems have been mounted to connect a separative technique (e.g., HPLC or GC)
 457 to a transmission cell and a FTIR detector (Vonach et al. 1997; Ahro et al. 2002;
 458 Kuligowski et al. 2010). Another modification in the cell is the inclusion of a heater
 459 to study the oxidative behavior of edible oils (Ismail et al. 2006), also used in NIR
 460 spectroscopy (Gonzaga and Pasquini 2006). The oxidation of edible oils has also
 461 been used in disposable cards, whose design is somewhat inspired by classic trans-
 462 mission cells.

[AU19] **Table 10.2** Commercial **FT-IR** sample cards and properties

Commercial name	Manufacturer/distributor	Film materials	Pathlength (μm)	
3M IR cards ^a	3M	PE ^b , PTFE ^c	10 and 100	t2.1 t2.2
PTFE and PTIR cards	International Crystal Laboratories	PE ^b , PTFE ^c	Unknown	t2.3 t2.4
Real Crystal IR cards	International Crystal Laboratories	NaCl, KBr, KCl	Unknown	t2.5
DOT-IR cards	PSI Performance Systematix	PTFE	Unknown	t2.6
ST-IR cards	Thermo Scientific ^d	PE, PTFE	~10	t2.7
^a Discontinued				t2.8
^b Polyethylene				t2.9
^c Polytetrafluoroethylene				t2.10
^d Initially commercialized by Thermo Nicolet				t2.11

10.3.2.2 Disposable IR Cards

Table 10.2 shows a summary of commercial **FTIR** cards. The disposable IR cards were developed in the 1990s by 3M for the analysis of liquids or spreadable fats. The cards are made up of a cardboard holder containing a circular IR-transmitting window made of a microporous substrate (polytetrafluoroethylene substrate for 4,000–1,300 cm⁻¹ or polyethylene substrate for 1,600–400 cm⁻¹ MIR analysis), although some manufacturers are commercializing cards of other materials. The sample is adsorbed on the microcrystalline pores of the film material, resulting in an effective path length of approximately 100 μm. The substrate bands of the microporous material can be subtracted from the sample spectra. A nonporous ring around the aperture prevents the sample from being absorbed by the cardholder. These cards were successfully applied to determine *trans* fatty acid content and the peroxide value (PV) of edible oils (Ma et al. 1998, 1999). Another type of IR cards (Type 2 STIR-PIR cards, Thermo-Nicolet) allows even shorter path lengths but lacks the nonporous ring around the aperture, and in consequence there is not consistency over time.

An improved version of these IR cards is the IR mesh cell (García-González and van de Voort 2009) (Fig. 10.9). Although it can be used for general applications, this cell is particularly adequate for running oxidation at moderate temperatures in a wide variety of conditions. The design of this new cell enables one to obtain a fairly consistent path length during the entire time of the experiment. This cell is endowed with a mesh that entraps the oil sample by means of its inherent surface tension. The high surface area provided by the mesh facilitates the rapid oxidation of the oil by air at ambient or slightly elevated temperatures with no need of extreme temperature conditions. These mesh cells are not disposable and can be easily cleaned and reused. Although the effective path length is fairly consistent over the course of the experiment, small changes in the sample thickness can be corrected using the CH combination band region (4,500–4,100 cm⁻¹) as a reference band (García-Gonzalez and van de Voort 2009). This band provides information on the CH double bonds and, thus, on the amount of sample and the OPL. This normalization procedure makes it possible to obtain reproducible spectra despite the small changes in the OPL

[AU20]

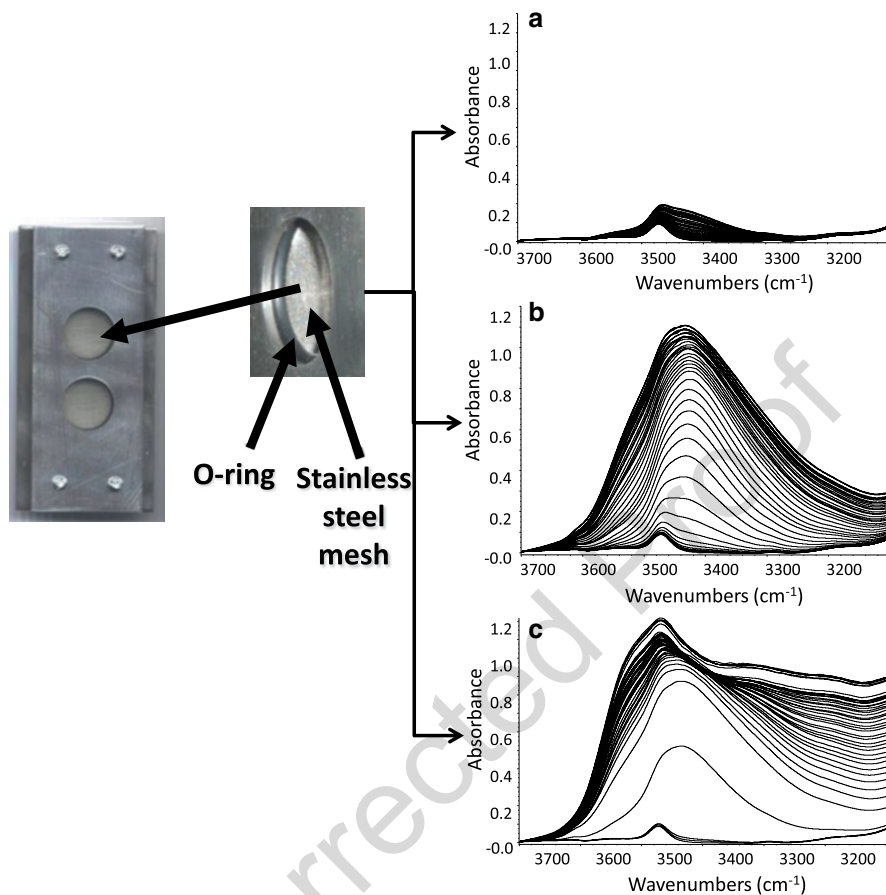


Fig. 10.9 Design of stainless steel mesh cell for infrared spectroscopy and spectra on OH stretching region ($3,700\text{--}3,100\text{ cm}^{-1}$) for canola oil in a mesh cell over a period of 42 days kept in the dark (a), exposed to room light (b), and heated at $50\text{ }^{\circ}\text{C}$ (c) (Permission of Applied Spectroscopy 2009 63:518–527)

494 over time or between different mesh cells. Thus, Fig. 10.10 shows the significant
 495 improvement in *trans* fatty acid calibration when the spectra have undergone nor-
 496 malization by the CH combination band.

497 10.3.2.3 Attenuated Total Reflection

498 Methods based on the ATR principle are available in a diverse range of configura-
 499 tions and optical designs. They typically require minimal sample presentation and
 500 are particularly suited to study highly absorbing samples such as edible oils. The
 501 spectral information arises from the interaction between the sample and the

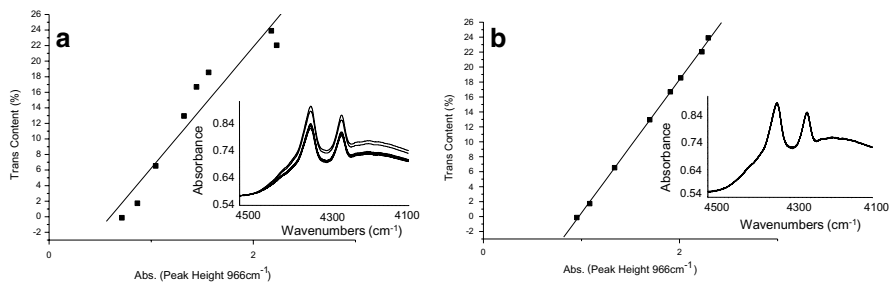


Fig. 10.10 Regression lines relating *trans* fatty acid content and peak height of 966 cm^{-1} band. (a) Data without normalization; (b) data normalized using CH overtone band at 4,334 cm^{-1} (shown in each panel as an inset) (Permission of Applied Spectroscopy 2009 63:518–527)

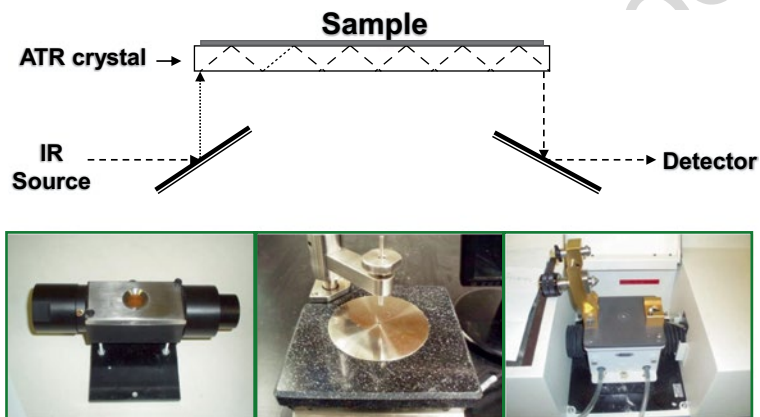


Fig. 10.11 Scheme of working principle of attenuated total reflection (ATR) and three pictures of typical ATR accessories

evanescent wave produced in an internal reflectance element (IRE). Infrared light is sent to the crystal at such an angle that it becomes internally reflected. Figure 10.11 shows a scheme of the working principle as well as some examples of ATR accessories, either multibounce or single-bounce (depending on the number of beam reflections within the ATR crystal).

Depending on the geometry and length of the crystal, the light will undergo multiple reflections before emerging from the crystal. At each reflection an evanescent wave is established that decays exponentially into the medium in contact with the crystal. If this medium is absorbing, then there will be a transfer of energy from inside the crystal to the surrounding medium and the emerging beam will be attenuated. ATR does not rely on the sample, which constitutes the surrounding medium, which is transparent or transmitting in the conventional sense (Harrick 1967).

502
503
504
505
506
507
508
509
510
511
512
513

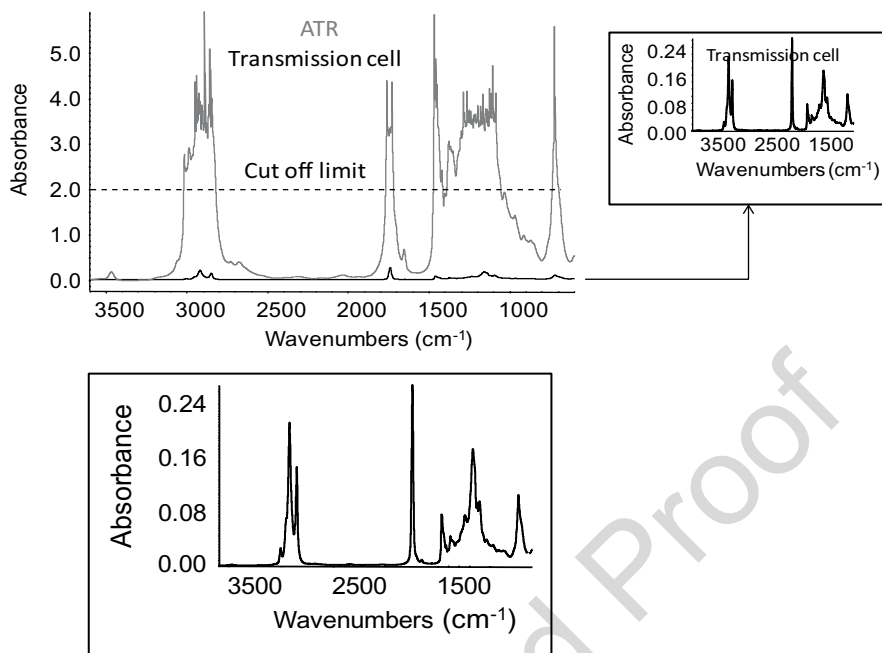


Fig. 10.12 Spectra of an oil collected with an ATR accessory and a transmission cell

514 ATR allows opaque or highly scattering samples to be used; the only proviso is
 515 that the sample must make intimate contact with the ATR crystal. This condition is
 516 fully completed with oil samples. The effective penetration (OPL) at any reflection
 517 is very short, typically a few microns, so that ATR can be used to overcome the
 518 strong absorption of materials. Thus, unlike the spectra obtained with transmission
 519 cells, ATR spectra have no cutoff limit or saturation problem and is suitable to study
 520 the whole spectra including the most intense bands (Fig. 10.12). A short effective
 521 path length is obtained with no restrictions on the sample thickness, so the sample
 522 is simply poured onto the ATR crystal. The optical paths are very reproducible from
 523 one sample to another. ATR then allows easy sample measurement, which is one
 524 reason that there has been an upsurge in interest in the MIR region (Wilson 1990).
 525 ATR crystals should be constructed from a material with a high refractive index,
 526 which is highly transmitting, inert, robust, easily cleaned, and resilient to abrasion
 527 and corrosion (including dissolution). Classically horizontal ZnSe, Ge, Si, or dia-
 528 mond crystals with 1, 6, or 12 internal reflections are used in oil analysis (van de
 529 Voort 1994a; Baeten et al. 2005; Abbas et al. 2009). Some disadvantages of ATR
 530 analysis are the low sensitivity because of the short effective path length (weak
 531 bands need to be studied with transmission cells), the significant effect that con-
 532 taminations on the crystal might have on the collected spectra, and the need for
 533 temperature control (the depth of penetration of the IR beam depends on tempera-
 534 ture) (Ismail et al. 2006).

10.3.3 Raman Spectroscopy

535

In the past, the application of Raman spectroscopy in food science was considered to be of very limited use because of fluorescence interference, photodecomposition, wavelength calibration, lack of precise frequency base from scan to scan, and the difficulty of attaining high-resolution spectra with the classic dispersive Raman spectrometer (Chase 1987). However, major instrumental advances have contributed to the widespread use of Raman spectroscopy in recent years (Gerrard and Birnie 1992) and its application in food science (Ozaki et al. 1992; Keller et al. 1993; Li-Chan 1996, 2010a).

536
537
538
539
540
541
542
543

First was the demonstration, by Hirschfeld and Chase in 1986, that Raman spectra could be obtained with a FT spectrometer equipped with a Nd:YAG laser (NIR monochromatic light excitation), a Rayleigh rejection filter, and a germanium detector. Later on, the development of compact and reliable diode lasers improved the quality of the commercially available systems. A third contribution to these developments was the use of low-noise, multichannel CCD detectors. By coupling the appropriate laser and a CCD detector to a spectrograph, it is now possible to measure Raman spectra in a few seconds without exciting fluorescence. Commercial FT-Raman spectrometers offer a good signal-to-noise ratio, a high IR-light throughput, rapid analysis, and the accuracy of wavelength calibration (Levin and Lewis 1990; Diem 1993; Schrader 1996; Li-Chan et al. 2010a).

544
545
546
547
548
549
550
551
552
553
554

[AU21]

FT-Raman spectroscopy is arguably the most versatile and easy-to-use nondestructive analytical procedure developed. In fact, glass and water have a very weak Raman spectrum, making the technique even easier to use. Samples can be measured directly in the bottle in the case of an oil. In addition, a spherical cell, such as a nuclear magnetic resonance (NMR) tube, allows Raman scattering information to be collected easily and rapidly (Schrader 1996). On the other hand, if samples to be investigated cannot be transported to the spectrometer, then optical fibers can be used (as in NIR spectroscopy). In the range of FT-Raman spectroscopy, quartz fibers have very high transmittance (Lewis et al. 1988; Hendra et al. 1997).

555
556
557
558
559
560
561
562
563

10.3.4 Fluorescence Spectroscopy

564

Fluorescence spectroscopy, like other vibrational spectroscopic techniques, is characterized by its simplicity of sample presentation. To obtain a fluorescence spectrum, it is necessary to excite a sample with an energy-specific excitation wavelength (λ_{ex}), which comes from an excitation source, passes through a filter or monochromator, and strikes the sample. Then a fluorescent light is emitted in all directions. Some of this fluorescent light passes through a second filter or monochromator, dividing the light into different emission wavelengths (λ_{em}), which reach a detector.

565
566
567
568
569
570
571

There are two general types of instruments: filter fluorometers, which use filters to isolate the incident light and fluorescent light, and the most common spectrofluorometers, which use diffraction grating monochromators to isolate the incident

572
573
574

575 light. Both types of instrument are composed of excitation sources, normally a
576 xenon lamp, filter or monochromator in excitation, filter or monochromator in emis-
577 sion, and a detector. The detector is usually placed at 90° to the incident light beam
578 to minimize the risk of transmitted or reflected incident light reaching the detector.
579 The detectors can be classified as single-channel or multichannel. The difference
580 between them is based on the number of wavelengths that they can detect at a time.
581 Thus, the single-channel detector can only detect the intensity of one wavelength at
582 a time. In contrast, the multichannel type detects the intensity at all wavelengths
583 simultaneously.

584 Various light sources may be used as excitation sources, including lasers, photo-
585 diodes, and lamps such as xenon arcs and mercury-vapor lamps. Of these, only the
586 xenon arc lamp has a continuous emission spectrum, with nearly constant intensity
587 in the range of 300–800 nm and a sufficient irradiance for measurements down to
588 just above 200 nm.

589 The most common accessory used to analyze the fluorescence spectrum of liquid
590 samples, and vegetable oils in particular, are quartz cuvettes with different paths,
591 internal widths, and volumes.

592 In addition to the conventional collection of emission spectra with a single exci-
593 tation wavelength, some fluorometers can be adapted to conduct analyses under two
594 particular modes that provide some advantages over the conventional mode. These
595 particular ways of measuring are commonly known as excitation-emission fluores-
596 cence spectroscopy (EEFS) and synchronic fluorescence spectroscopy (SFS).

597 **10.3.4.1 Excitation-Emission Fluorescence Spectroscopy (EEFS)**

598 EEFS consists in measuring the emission spectra at different excitation wave-
599 lengths (λ_{ex}). The result of this measurement is a three-dimensional (3D)
600 excitation-emission matrix (EEM). Compared to conventional fluorescence spec-
601 troscopy, this technique improves the selectivity of the method. Its main advan-
602 tage is that it enables obtaining simultaneous information about the different
603 fluorophores present in a sample. Furthermore, EEFS is useful for selecting the
604 most convenient excitation wavelengths to study specific fluorescent compounds
605 in complex matrices by conventional fluorescence spectroscopy. The measure-
606 ments under this mode also have some disadvantages. The spectroscopic param-
607 eters must be optimized beforehand to avoid Rayleigh scattering caused as a result
608 of the overlap between the ranges of wavelengths of excitation and emission. As a
609 drawback, this mode consumes a longer analysis time to obtain a matrix (EEM),
610 approximately 10 min depending on the spectral ranges used. The statistical data
611 treatment is also more sophisticated or requires a preliminary decomposition of
612 the information EEM in two-dimensional arrays. For this purpose, parallel factor
613 analysis (PARAFAC) is an appropriate way to decompose and interpret 3D data
614 matrices (Tena et al. 2012).

10.3.4.2 Synchronous Fluorescence Spectroscopy (SFS)

615

This technique consists in scanning the signal of two monochromators, the excitation and emission, simultaneously, keeping a constant interval of wavelengths ($\Delta\lambda$) between excitation (λ_{ex}) and emission (λ_{em}) wavelengths. Three types of SFS procedures can be distinguished depending on the scan rate: (1) constant-wavelength SFS, where the interval wavelength ($\Delta\lambda$) between λ_{ex} and λ_{em} is kept constant; this is the most widely used SFS procedure; (2) constant-energy SFS, where a frequency difference ($\Delta\nu$) is kept constant; (3) variable-angle SFS, where the excitation and emission wavelengths may be varied simultaneously but at different rates. These last two types are more difficult to implement, mostly because commercial fluorimeters are not endowed with the necessary software for such scans. Thus, a regular fluorimeter typically only allows a constant-wavelength SFS. The selection of $\Delta\lambda$ depends on which fluorophore compounds comprise the analytical targets of the study. Most of the reviewed literature on SFS indicates that 3D rendering helps in obtaining a better characterization of multifluorophore systems. The resulting 3D surfaces are obtained when the ZZ' axis is represented – the different wavelength intervals ($\Delta\lambda$) used in the course of the experiments – versus the XX' axis, which represents the range of synchronous wavelengths scanned. This graph is used to determine which $\Delta\lambda$ is the most appropriate for obtaining more information about particular spectral bands.

One advantage of total SFS is the narrowing of the bands, which simplifies the spectrum by minimizing the spectral overlap. This narrowing of bands depends on the selected wavelength interval ($\Delta\lambda$). The high selectivity of the total synchronous fluorescence spectra makes this technique suitable for the qualitative analysis of complex samples. The main disadvantages of this mode are the difficulty of selecting an appropriate $\Delta\lambda$ in the case of multicomponent samples and the requirement of specific instrumentation and software to take full advantage of the technique (monochromator plus driving software).

10.3.5 Online Analysis

643

In the food industry, monitoring of the process is a major issue in order to optimize it and to assure the quality of the end products. To this end, at-line or online analytical methods can be applied. With at-line methods, samples are taken from the process line and analyzed close to it or in a laboratory. At-line methods are time-consuming and do not allow one to obtain the required information in due time in order to act rapidly (or even instantaneous) on the process. Online methods, where the instrument is directly installed in the process line, is more appropriate for process monitoring. NIR, MIR, and Raman spectroscopy are techniques that are suitable for providing real-time measurements that can be integrated into an industrial

653 process. Recent developments have been observed mainly in the setup of adequate
654 sensors and software allowing the collecting of spectral information and to use it to
655 pilot food processes. Online NIR spectroscopy has several advantages, such as
656 speed of measurement, well-developed equipment and devices, absence of a need
657 for sample preparation as well as analysis of simultaneous parameters. The main
658 disadvantage is the need for robust calibrations and model transfer between instru-
659 ments (Kondepoti and Heise 2008). The online applications of NIR in food systems
660 have recently increased significantly. Huang et al. (2008) published a review on
661 NIR online analysis of foods such as meat, fruit, grain, dairy products, and bever-
662 ages. Online MIR spectroscopy is less frequently used in the food industry but has
663 several advantages over NIR spectroscopy such as high sensitivity, ability to distin-
664 guish between very similar structures, and good calibration transfer between
665 instruments. Online MIR application suffers mainly from the strong absorption of
666 water and the high cost (e.g., fiber optics suitable for MIR analysis are more expen-
667 sive and less adapted for online control than those suitable for NIR analysis). Few
668 studies on the use of MIR for online applications, such as monitoring a fermenta-
669 tion reaction, have been reported (Bellon-Maurel et al. 1994; Fayolle et al. 2000).
670 Unlike MIR online spectroscopy, online Raman spectroscopy has few applications
671 in the food industry. However, it is commonly used in the pharmaceutical process-
672 ing industry.

673 Few papers dealing with online use of NIR spectroscopy for the control of [AU22]
674 olive oil, olive pomace, and olive paste have been published. One of the first pre-
675 liminary studies of the application of online NIR spectroscopic methods in this
676 field was published by Hermoso et al. (1999). In this paper, the NIR technique was
677 used to measure the oil content and humidity in olive pomace at the decanter. The
678 study provided determination coefficients of 0.91 and 0.6 between NIRS and the
679 reference values of oil content and humidity obtained by NMR and the drying-
680 oven method, respectively. In 2005, Jiménez-Márquez et al. applied NIR transmit-
681 tance spectroscopy to online control quality and characterization of virgin olive
682 oils. Partial least-squares (PLS) models were developed for acidity value, bitter
683 taste, and fatty acid composition. Gallardo-González et al. (2005) used NIR to
684 determine in real time the moisture and fat contents of olive pastes and the result-
685 ing olive wastes generated in the two-phase oil extraction process. Coefficients of
686 determination of 0.90 for humidity and 0.91 for oil content in olive paste samples
687 were obtained.

688 More recently, Cayuela et al. (2009, 2010) predicted olive fruit and virgin olive
689 oil quality parameters by directly measuring the fruit using NIR. The analyzed
690 parameters were free acidity in olive oil, oil yield from physical extraction, oil con-
691 tent referring to fresh weight, oil content referring to dry matter and fruit moisture.
692 The results indicated a very good predictive potential of the methodology and served
693 to encourage improvement in the obtained models through the enlargement of cali-
694 bration databases and models.

10.4 Data Acquisition

695

The data acquisition procedure in IR or Raman spectrometry is not tedious and can be done by nonskilled technicians. Basically, the principal steps are as follows: preliminary work for data acquisition (e.g., cool the detector with N₂ in Raman spectroscopy, heat the sample accessory in NIR or MIR spectroscopy), instrument performance verification, stabilization, and data collection. These steps are, for the most part, described in the technical manual supplied with the instrument. The performance of the instrument is generally checked by various automatic functions that are included in the program designed to control the spectrometer. However, before each experiment, it is appropriate to collect and store the spectrum of a defined standard (e.g., oil or chemical product defined as standard). In so doing, the spectral quality and the stability of the spectrometer can be verified each day.

The stabilization procedure is essential for acquiring a high-quality spectrum, i.e., a spectrum with a good signal-to-noise ratio. The manual of the instrument will contain the reference value normally reached by the spectrometer. To perform this work, the more convenient way is by successively collecting the spectral data of the same sample. It is important to do this collection under conditions that will be used in practice. The acquisition of a series of spectra before the analytical step allows, according to the analytical conditions, the stabilization of the instrumental components (e.g., source, detector). The analytical conditions include the number of scans to coadd and the resolution of the spectrum. The best way to define these parameters is to carry out a repeatability study, changing one of the parameters at a time. In comparison to simple univariate analysis, little progress has been made so far in the quantification of variability in multivariate analysis. Hence, it is judicious to complete the statistical results from the univariate analysis (SD and CV) with those from a multivariate procedure such as cluster analysis. Cluster analysis develops a mathematical model evaluating the similarities and dissimilarities between multivariate data (Massart and Kaufman 1983). A convenient agglomerative procedure and linkage distance in the analysis of spectroscopic data are Ward's method and the city-block (Manhattan) distance, respectively (Chap. 10). A low value of the linkage distance indicates a high similarity, i.e., a good repeatability.

When the instrument performance has been checked and the stability of the instrument achieved, the data collection procedure can be carried out. This step includes the reference spectrum acquisition, the sample spectrum acquisition, and sample-handling cleaning. The reference spectrum consists of the spectrum of the empty sample accessory or the spectrum of a reference compound (e.g., ceramic plate in NIR spectroscopy). This step permits the removal of absorbances due to the instrument and sample handling used from the sample. Depending on the technique and the sample accessory used, the reference spectrum should be collected once a day (e.g., NIR) or before each spectral data acquisition (e.g., ATR/FT-MIR). After the reference acquisition, the sample is introduced in the sample accessory and its spectrum is collected. Before the following data acquisition, the sample must be

696

697

698

699

700

701

702

703

704

705

706

707

708

709

710

711

712

713

714

715

716

717

718

719

720

721

722

723

724

725

726

727

728

729

730

731

732

733

734

735

736

737 removed and the accessory cleaned (this is not the case with automatic sampling
738 methods, as discussed in Sect. 10.3.2.). Then, the cleaned sample handling should
739 be spectrally checked to ensure that no residue from the previous sample remains.

740 10.5 Interpretation of Oil Spectra

741 The most frequently discussed drawback of spectroscopic techniques is the diffi-
742 culty of chemically interpreting the spectral data. Separative techniques like chro-
743 matography generate information (chromatograms) mainly containing well-resolved
744 and separate peaks, i.e., discrete information. Infrared and Raman spectroscopic
745 techniques generate continuous information (spectra) rich in both isolated and over-
746 lapping bands. While in chromatography each peak is, in general, characteristic of
747 a precise compound, in spectroscopy, the bands are the result of the vibration of one
748 or more chemical bonds (e.g., C-H, C=C) present in all the compounds constituting
749 the sample. Each band in the spectrum of a mixture contains the sum of the informa-
750 tion of various molecules.

751 To make up for the unreadable information on the IR and Raman spectra, it is
752 important to study the spectral features of pure chemical products. Edible oils
753 mainly contain triacylglycerols (TAGs) whose types and proportion vary according
754 to their source. Hence, the study of pure compounds such as TAGs (or fatty acid
755 methyl esters) allows the band assignment of the principal absorption (NIR, MIR)
756 or scattered (Raman) bands observed in the spectra. Various papers have presented
757 the spectral features of pure chemical products (Holman and Edmondson 1956;
758 Bailey and Horvat 1972; Sadeghi-Jorabchi et al. 1991; Sato et al. 1991; van de Voort
759 et al. 1994b; Hourant et al. 2000; Baeten et al. 2001; Stefanov et al. 2010). In addi-
760 tion, various companies offer spectral libraries containing the characteristic spectra
761 of the compounds concerned.

762 The analysis of various kinds of samples from different animal and vegetable
763 sources permits the interpretation of the most noteworthy bands. The correlation at
764 each frequency between the absorption (or scattering) intensity and chemical com-
765 pounds (or indices) can be calculated using the fatty acid profile determined by gas
766 chromatography. These correlation graphs help the analyst to underline the spectral
767 features of each oil source and guide the subsequent data analysis.

768 To present the main characteristics of NIR, MIR, and Raman spectra, the relevant
769 frequencies of pure chemical compounds will be presented and discussed later on. For
770 each technique, the principal correlated frequencies with the total amount of unsatu-
771 rated fatty acids ($\text{UFA} = \text{C16:1} + \text{C18:1} + \text{C18:2} + \text{C18:3}$), monounsaturated fatty acids
772 ($\text{MUFA} = \text{C16:1} + \text{C18:1}$), polyunsaturated fatty acids ($\text{PUFA} = \text{C18:2} + \text{C18:3}$), satu-
773 rated fatty acids ($\text{SFA} = \text{C6} + \text{C8} + \text{C10} + \text{C14} + \text{C16} + \text{C18}$), and iodine value ($\text{IV} = 1 * \text{C}$
774 $16:1 + 1 * \text{C18:1} + 2 * \text{C18:2} + 3 * \text{C18:3}$) are displayed in the next paragraph.

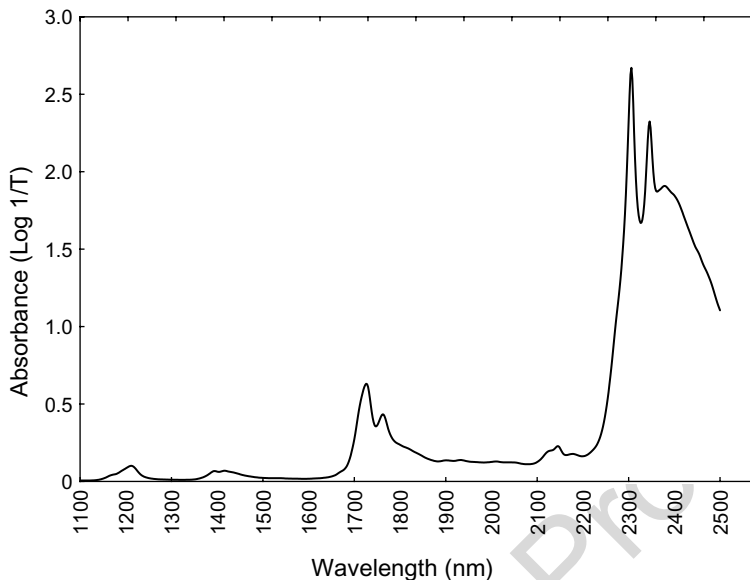


Fig. 10.13 Near-infrared spectrum of a virgin olive oil

10.5.1 Near-Infrared Spectra

775

NIR spectra show various overlapping peaks. As seen in the theory section, these bands are the result of overtones (first and second) and a combination of fundamental, largely hydrogenic, vibrations that occur in the MIR region. Various books and papers describe the assignment of the major NIR absorption bands (Holman and Edmondson 1956; Goddu 1957; Fenton and Crisler 1959; Williams and Norris 2001; Panford and deMan 1990; Sato et al. 1991; Sato 1994). Figure 10.13 and Table 10.3 display, respectively, the NIR spectrum (1,100–2,500 nm) obtained with a transmission cell and the assignment of the most noteworthy absorption bands of a virgin olive oil.

776
777
778
779
780
781
782
783
784

All studies that have used the NIR region of the electromagnetic spectra have shown that oil spectra contain information about the degree of unsaturation (IV) (Holman and Edmondson 1956), the total unsaturation (Goddu 1957), the carbon number (Wetzel 1983), and the composition of the unsaturated fraction (Sato et al. 1991). In addition, NIR spectra show specific information about *cis* isomers, while *trans* isomers have no noteworthy bands.

785
786
787
788
789
790

Sato et al. (1991) showed that mainly two regions of the NIR spectra have particular features (Table 10.4). First, an absorption intensity near 1,720 nm is characteristic of the first overtone of the C-H vibration of various chemical groups ($-\text{CH}_3$, $-\text{CH}_2$, $=\text{CH}-$) and varies according to analyzed TAGs. In fact, as the degree of

791
792
793
794

t3.1 **Table 10.3** Assignment of most noteworthy near-infrared absorption
t3.2 bands of a virgin olive oil spectrum

t3.3	Wavelength (nm)	Molecule	Group	Vibration
t3.4	1,090–1,180	-CH ₂	C-H	Second overtone
t3.5	1,100–1,200	-CH ₃	C-H	Second overtone
t3.6	1,150–1,260	-CH=CH-	C-H	First overtone
t3.7	1,350–1,430	-CH ₂	C-H	Combination
t3.8	1,360–1,420	-CH ₃	C-H	Combination
t3.9	1,390–1,450	H ₂ O	O-H	First overtone
t3.10	1,650–1,780	-CH ₂	C-H	First overtone
t3.11		-CH ₃	C-H	First overtone
t3.12		-CH=CH-	C-H	First overtone
t3.13	1,880–1,930	H ₂ O	O-H	Combination
t3.14	2,010–2,020	-CH=CH-	C-H	Combination
t3.15	2,100–2,200	-CH=CH-	C-H	Combination
t3.16	2,240–2,360	-CH ₃	C-H	Combination
t3.17	2,290–2,470	-CH ₂	C-H	Combination

t4.1 **Table 10.4** Relevant near-infrared wavelengths (nm) of several lipids and bands that are correlated
t4.2 with some chemical indices ($R > 0.90$)

		Spectral region		
t4.3	Lipids	Second overtone	First overtone	Combination
t4.4	Tricaprin (C10:0)		1,726, 1,800	2,128
t4.5	Triolein (<i>cis</i> C18:1)		1,725	2,143
t4.6	Trilinolein (<i>cis</i> C18:2)		1,665, 1,717	2,143
t4.7	Trilinoelaidin (<i>trans</i> C18:2)		1,725, 1,800	2,131
t4.8	Trilinolenin (<i>cis</i> C18:3)		1,665, 1,712	2,143
t4.9	MUFA		1,724, 1,766	2,358
t4.10	PUFA	1,162, 1,212 ^a	1,660, 1,698, 1,730 ^a	2,136, 2,176, 2,224, 2,310 ^a , 2,348 ^a , 2,434 ^a
t4.11				
t4.12	IV	1,164	1,664, 1,714,	2,144, 2,178, 2,340 ^a ,
t4.13			1,740 ^a , 1,784 ^a	2,444 ^a

t4.14 *UFA* unsaturated fatty acids, *MUFA* monounsaturated fatty acids, *PUFA* polyunsaturated fatty
t4.15 acids, *SFA* saturated fatty acids, *IV* iodine value

t4.16 ^anegative correlation coefficient

795 unsaturation increases, the maximum point observed in the spectra of triolein at
796 1,725 nm shifts to 1,717 nm and 1,712 nm in spectra of trilinolein and trilinolenin,
797 respectively. Second, the absorption band in the area of 2,143 nm, characteristic of
798 the C-H vibration of *cis*-unsaturation, is more intense in polyunsaturated than in
799 monounsaturated fatty acid spectra. Saturated and *trans* fatty acids show weak
800 peaks and with maxima in the vicinity of 2,128 and 2,131 nm. Wavelengths in the
801 region of 1,800 nm seem to be characteristic of saturated fatty acids.

802 A study of 104 samples from 18 different sources (animal and vegetable) showed
803 that the spectral features of oils and fats agree with their fatty acid composition as

Table 10.5 Assignment of most noteworthy mid-infrared bands of a virgin olive oil spectrum

Wavenumber (cm ⁻¹)	Molecule	Group	Vibration	
3,007	<i>cis</i> -CH=CH-	C-H	ν	15.1
2,955	-CH ₃	C-H	ν	15.2
2,924	-CH ₂	C-H	ν	15.3
2,855	-CH ₂ and -CH ₃	C-H	ν	15.4
1,746	-C=O	C=O	ν	15.5
1,653	<i>cis</i> -CH=CH-	C=C	ν	15.6
1,462	-CH ₂	C-H	δ	15.7
1,377	-CH ₃	C-H	δ	15.8
1,236	-CH ₂	C-H	δ	15.9
1,300–800	Carbon skeleton	C-C	δ	15.10
1,200–1,000	-CO-O-	C-O	δ	15.11
990–960	<i>trans</i> -CH=CH-	C-H	δ	15.12
723	-CH ₂	C-H	δ	15.13
ν stretching, δ deformation				15.17

determined by gas chromatography (Hourant 1995; Hourant et al. 2000). Oils with a high amount of polyunsaturated fatty acids have a maximum absorption band at lower wavelengths in the vicinity of 1,720 nm. Moreover, they have higher absorbance intensity, in the vicinity of 1,720 and 2,140 nm, than oils rich in monounsaturated fatty acids. Sunflower, walnut, and soybean oils present a maximum intensity near 1,720 nm, corn and rapeseed oils near 1,722 nm, and peanut, high oleic sunflower, and olive oils in the vicinity of 1,724 nm. The spectral regions 1,100–1,300 and 2,050–2,230 nm also show spectral features characteristic of these vegetable species. Table 10.4 regroups the wavelengths showing a high coefficient of correlation (greater than 0.90) between the absorption intensities and different chemical indices.

10.5.2 Mid-Infrared Spectra

A MIR spectrum of vegetable oil contains well-resolved peaks (3,100–1,700 cm⁻¹) and overlapping peaks (fingerprint region, 1,500–700 cm⁻¹) whose assignment is more difficult (Socrates 1994). Figure 10.4 displays the MIR spectrum of virgin olive oil, while Table 10.5 shows its most noteworthy bands (Fig. 10.14).

Based on the information contained in the MIR spectra, a series of methods has been developed to quantify the *trans* content (AOCS 1988; Sleeter and Matlock 1989; Ulberth and Haider 1992; van de Voort et al. 1995; Mossoba et al. 1996; Ratnayake and Pelletier 1996), the *cis* content (van de Voort et al. 1995), the peroxide content (van de Voort et al. 1994b), the aldehyde content in thermally stressed oils (Dubois et al. 1996), and the free fatty acid content (Ismail et al. 1993). MIR spectroscopy was also used in the determination of indices such as the anisidine

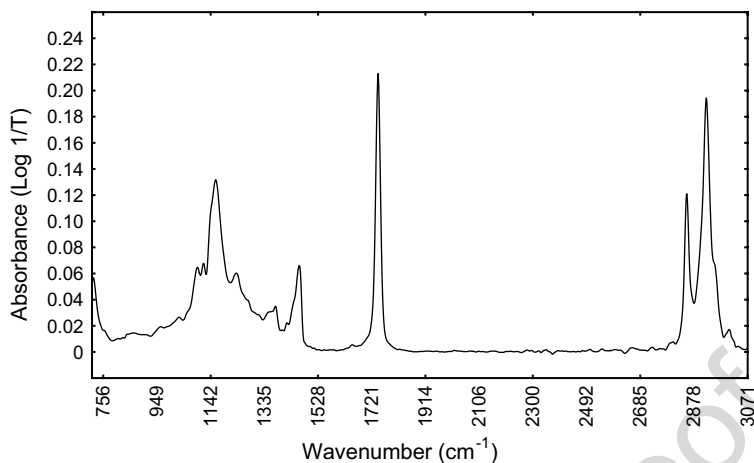


Fig. 10.14 FT-mid-infrared spectrum of a virgin olive oil

827 value (Dubois et al. 1996), iodine value (Afran and Newberry 1991; Muniategui
 828 et al. 1992; van de Voort et al. 1992), saponification number (van de Voort et al.
 829 1992), and the solid fat index (van de Voort et al. 1996).

830 The investigation of pure fatty acids underlines the fact that spectral features
 831 change with the degree of unsaturation (van de Voort et al. 1995). The C-H stretch-
 832 ing vibration of $-\text{CH}_2$ and $-\text{CH}_3$ groups ($2,950\text{--}2,800\text{ cm}^{-1}$), the C=O stretching
 833 vibration of carbonyl groups ($1,745\text{ cm}^{-1}$), and the C-H bending vibration of $-\text{CH}_2$
 834 and $-\text{CH}_3$ groups ($1,400\text{--}1,200\text{ cm}^{-1}$) have absorption band intensities that change
 835 with the degree of unsaturation of the lipid matter. Moreover, the peak centered near
 836 $3,005\text{ cm}^{-1}$ (C-H stretching vibration of *cis* $-\text{CH}=\text{CH}-$) in the spectrum of triolein
 837 shifts to higher frequency in the trilinolein ($3,010\text{ cm}^{-1}$) and trilinolenin ($3,012\text{ cm}^{-1}$)
 838 spectra as the degree of unsaturation rises (Table 10.4). On the other hand, *trans*
 839 fatty acids show a peak centered near $3,025\text{ cm}^{-1}$.

840 The fingerprint region of pure fatty acids is rich in features indicative of the
 841 degree of unsaturation, the type of unsaturation (mono- or polyunsaturated), or the
 842 content of *cis* and *trans* isomers. In a range from $1,125$ to $1,095\text{ cm}^{-1}$ (characteristic
 843 of C-O and C-C stretching vibration), the peak intensities and the shape of the spec-
 844 tra vary with the unsaturation of fatty acids.

845 A study of 64 samples from 13 sources revealed that certain absorption bands of
 846 oil spectra vary with their fatty composition (Hourant 1995). The weak peak near
 847 $3,010\text{ cm}^{-1}$ has a higher intensity as the major fatty acids in the sample are monoun-
 848 saturated or polyunsaturated. Moreover, samples rich in C18:1 (e.g., olive oil) have
 849 higher absorbance near $2,953$ and $2,922\text{ cm}^{-1}$ than those rich in C18:2.

850 However, the most important spectral features appear in the fingerprint region.
 851 Two bands near $1,121$ and $1,098\text{ cm}^{-1}$ show interesting spectral features. The absor-
 852 bance intensity in the vicinity of $1,121\text{ cm}^{-1}$ shows a positive correlation with the
 853 amount of oleic acid, while the intensity near $1,098\text{ cm}^{-1}$ is correlated with the

Table 10.6 Relevant mid-infrared wavenumbers (cm^{-1}) of several lipids and bands that are correlated with some chemical indices ($R > 0.90$)

Lipids	Spectral region		
	= C-H stretching	Fingerprint region	
Tristearic (C18:0)	–	–	t6.3
Triolein (<i>cis</i> C18:1)	3,005	913	t6.4
Trielaidin (<i>trans</i> C18:1)	3,025	966	t6.5
Trilinolein (<i>cis</i> C18:2)	3,010	913	t6.6
Trilinoelaidin (<i>trans</i> C18:2)	3,025	968	t6.7
Trilinolenin (<i>cis</i> C18:3)	3,012	913	t6.8
MUFA	3,011, 2,964	1,425, 1,396, 1,273, 1,134, 1,101, 914	t6.9
PUFA	2,924, 2,854	1,464, 1,408, 1,313, 1,118	t6.10
IV	3,011, 2,965, 2,922 ^a , 2,853 ^a	1,429, 1,395, 1,267, 1,132, 1,117 ^a , 1,098, 922	t6.11
<i>UFA</i> unsaturated fatty acids, <i>MUFA</i> monounsaturated fatty acids, <i>PUFA</i> polyunsaturated fatty acids, <i>SFA</i> saturated fatty acids, <i>IV</i> iodine value			t6.12
^a negative correlation coefficient			t6.13

amount of linoleic acid (Aparicio and Baeten 1997). In addition, the peak centered at 913 cm^{-1} is not present (or is very weak) in high oleic sunflower and olive oil, while it is more intense in samples rich in polyunsaturated fatty acids. Table 10.6 shows the wavenumbers with a coefficient of correlation between the absorption intensities and different chemical indices higher than 0.90. The region near $3,010\text{--}2,950 \text{ cm}^{-1}$ and the fingerprint region ($1,500\text{--}700 \text{ cm}^{-1}$) show the highest correlation with the different indices in relation to the degree of unsaturation of the samples.

10.5.3 Raman Spectra

The spectra of edible fats and oils obtained by FT-Raman spectrometers contain well-resolved bands with various scattering intensities and shapes. The spectra show good signal-to-noise ratios and contain information from different vibrational bands (stretching and bending) of various chemical groups. Raman scattering arises from the change in the polarizability or shape of the electron distribution in the molecule as it vibrates, while, in contrast, IR absorption requires a change in the intrinsic dipole moment with the molecular vibration (Grasseli and Bulkin 1991). Hence, polar groups (such as C=O and O-H) have strong MIR absorption bands, whereas nonpolar groups (such as C=C) show intense Raman scattered bands. Because the main feature of unsaturated fatty acids is their content of double bonds and their configuration (*cis* or *trans*), FT-Raman spectra are of great value in the study of lipids. Raman spectroscopy has been used in the determination of the total amount of unsaturation (iodine value) and of the *cis/trans* isomer content of edible oils (Bailey and Horvat 1972; Sadeghi-Jorabchi et al. 1990, 1991). Figure 10.15 and Table 10.7 display respectively the FT-Raman spectrum and the assignment of the most noteworthy bands of a virgin olive oil.

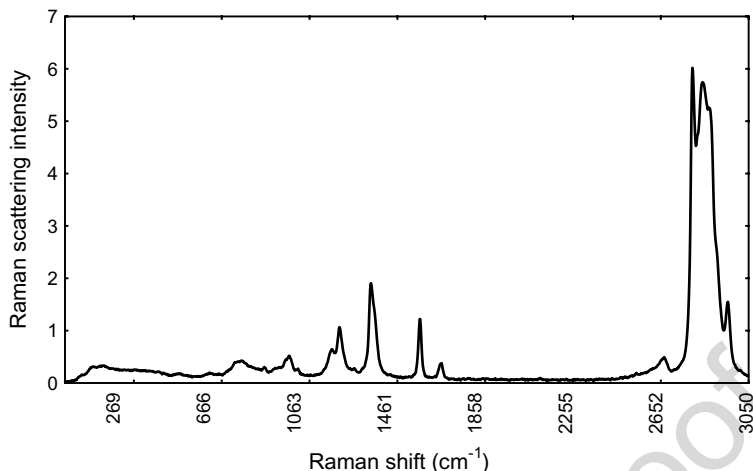


Fig. 10.15 FT-Raman spectrum of a virgin olive oil

t7.1 **Table 10.7** Assignment of most noteworthy Raman scattering bands of a
t7.2 virgin olive oil spectrum

t7.3	Raman shift (cm ⁻¹)	Molecule	Group	Vibration
t7.4	3,007	RCH=CHR	=C-H	ν
t7.5	2,926	-CH ₂	C-H	ν
t7.6	2,897	-CH ₃	C-H	ν
t7.7	2,855	-CH ₂	C-H	ν
t7.8	1,748	RC=OOR	C=O	ν
t7.9	1,670	<i>trans</i> RCH=CHR	C=C	ν
t7.10	1,655	<i>cis</i> RCH=CHR	C=C	ν
t7.11	1,441	-CH ₂	C-H	δ
t7.12	1,306	-CH ₂	C-H	δ
t7.13	1,270	<i>cis</i> RCH=CHR	=C-H	δ
t7.14	1,100–1,000	-(CH ₂) _n -	C-C	ν
t7.15	900–800	-(CH ₂) _n -	C-C	ν

t7.16 ν stretching, δ deformation

878 Bailey and Horvat (1972) studied the spectral features in the area of 1,660 cm⁻¹
879 (C=C stretching vibration) of triolein, trielaidin, trilinolein, and trilinolenin. In
880 this region, *trans* isomers had a peak centered near 1,670 cm⁻¹, while *cis* isomers
881 showed a peak in the vicinity of 1,660 cm⁻¹. Later on, Sadeghi-Jorabchi et al.
882 (1991) studied and underlined other characteristics of pure methyl esters in their
883 work on the quantification of *cis* and *trans* content by FT-Raman spectroscopy.
884 They showed the particular features of fatty acids near 3,010 (=C-H stretching
885 vibration) and 1,270 cm⁻¹(=C-H bending vibration). In the area of 3,010 cm⁻¹ a

Table 10.8 Relevant Raman shifts (cm^{-1}) of several lipids and bands that are correlated with some chemical indices ($R > 0.90$)

Lipids	Spectral region			
	= C-H stretching	C=C stretching	C-H bending	
Methyl oleate (<i>cis</i> C18:1)	3,006	1,654	1,439, 1,267	t8.3
Methyl elaidate (<i>trans</i> C18:1)	2,995	1,667	1,439	t8.4
Methyl linoleate (<i>cis</i> C18:2)	3,011	1,657	1,440, 1,265	t8.5
Methyl linolenate (<i>cis</i> C18:3)	3,013	1,657	1,441, 1,266	t8.6
MUFA	2,890, 2,874 ^a , 2,845			t8.7
PUFA	3,021, 2,922, 2,884 ^a , 2,870, 2,855 ^a	1,667, 1,642	1,256	t8.8
IV	3,007, 2,991, 2,911, 2,882 ^a , 2,855 ^a	1,657, 1,646	1,268	t8.9
UFA unsaturated fatty acids, MUFA monounsaturated fatty acids, PUFA polyunsaturated fatty acids, SFA saturated fatty acids, IV iodine value				t8.10
^a negative correlation coefficient				t8.11
				t8.12
				t8.13

shift to a higher frequency and an increase in the scattering intensities occurs as the degree of unsaturation rises. Similar observations were reported at 1,660 and 1,270 cm^{-1} . Table 10.6 shows the main characteristics of various methyl esters.

The region near 3,010 cm^{-1} is particularly affected by the major fatty acid components (Baeten et al. 1998). In fact, samples relatively rich in polyunsaturated fatty acids (e.g., corn, sunflower, and sesame oils) had a more intense scattering band and a higher frequency maximum than samples rich in monounsaturated fatty acids (e.g., olive oil). This band is also important in the authentication of olive oil (Baeten et al. 1996). The usefulness of Raman shifts in the range 2,880–2,840 cm^{-1} (C-H stretching vibration of CH_2 and CH_3) for varietal discrimination has also been noted (Aparicio and Baeten 1998). In this region, samples rich in polyunsaturated fatty acids (e.g., rapeseed, sunflower, and walnut oils) have weaker scattering intensities than those that have a high content of monounsaturated fatty acids (e.g., olive oil).

The region of 1,660 and 1,265 cm^{-1} is also characteristic of the fatty acid profile of the fat or oil variety studied. Samples rich in polyunsaturated fatty acids such as walnut, sunflower, corn, and sesame oils have a maximum near 1,657 cm^{-1} , while olive and high oleic sunflower show a maximum near 1,655 cm^{-1} . The intensity at these Raman shifts rises with the degree of unsaturation. Near 1,259 cm^{-1} , the scattering intensities increase as the degree of unsaturation decreases. The fingerprint region (1,100–700 cm^{-1}) of pure methyl esters and of different oil varieties also have information (Sadeghi-Jorabchi et al. 1991). However, the poor signal-to-noise ratio at these frequencies does not allow, at the moment, evaluation of the information. Table 10.8 regroups the wavenumbers showing a maximum coefficient of correlation between the absorption intensities and different chemical indices.

10.5.4 Fluorescence Spectra

Vegetable oils are commonly analyzed by fluorescence spectroscopy untreated or diluted at 1 % in hexano v/v. In particular, Fig. 10.16 displays the fluorescence

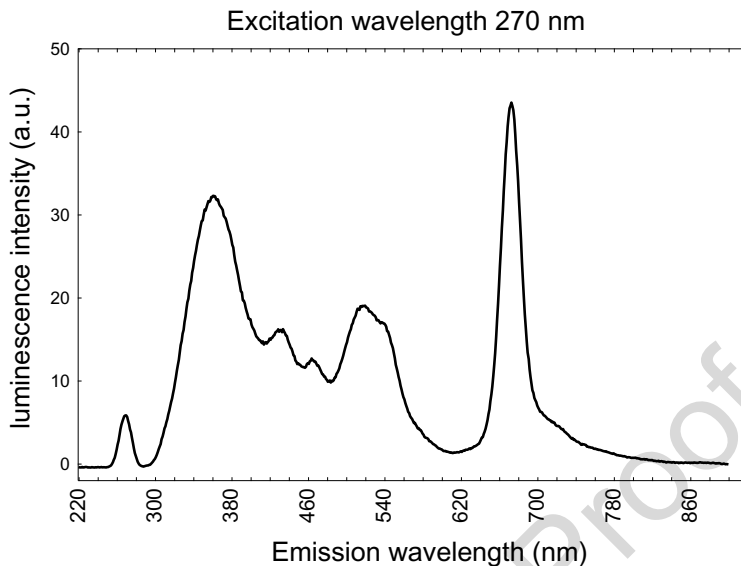


Fig. 10.16 Fluorescence spectra of a virgin olive oil

913 spectrum of a virgin olive oil in its native form (nondiluted). The bands observed in
914 this spectrum have been related to species that are shown in Table 10.9. In this table
915 also appears the emission wavelength of these fluorophores. The spectral profile and
916 the intensities of these bands dramatically vary with the oxidation degree of the
917 samples, as was shown in Fig. 10.3. The bands of some fluorescent compounds,
918 such as chlorophylls, are more intense than other fluorescent species, although the
919 intensity greatly depends on the excitation wavelength. The magnitude of this peak
920 with respect to others may cause problems when handling the whole data set. This
921 problem can be avoided by studying narrower ranges of wavelengths instead of
922 processing the information of the entire emission spectra.

923 10.6 Data Treatment

924 The main analytical problem with spectroscopic data is to extract the information in
925 such a way that it can be used in quantitative analysis. IR and Raman spectra are
926 usually the mean of various coadded spectra (normally between 100 and 200). The
927 collection of a high number of coadded spectra is allowed by the rapidity of the
928 acquisition of a single coadded spectrum in an FT instrument (around a few sec-
929 onds). The spectra displayed throughout the present chapter are coadded spectra.
930 These spectra are a rich source of multivariate data (more than 700 data points)
931 where each frequency represents a variable. Various strategies have been proposed

Table 10.9 Emission wavelength associated with fluorophores present in olive oil

Fluorescent compounds	λ_{em} (nm)	Reference
Pigment (chlorophylls and pheophytins)	692–765	Sayago et al. (2007)
α -, β -, and γ -tocopherols, phenols	275–400	Dupuy et al. (2005)
Chlorophyll a and b, pheophytin a and b	600–700	
Oxidized products from vitamin E	400–600	
Tocopherols and tocotrienols	300–350	Sikorska et al. (2005)
Chlorophylls and pheophytins	660–700	
Oxidized product	400	
Phenols	300–390	Zandomenighi et al. (2005)
Chlorophylls and derivatives	640–800	
Tocopherols	328	Giungato et al. (2004)
Chlorophyll a	669	
Parinaric acid isomerization	406	
Vitamin E (oxidized products)	440, 475, 525	Guimet et al. (2004)
Chlorophylls	650 y 700	
Chlorophyll a	669	Galeano et al. (2003)
Chlorophyll b	653	
Pheophytin a	671	
Pheophytin b	658	
Hydroxyl radical	452,3	Tai et al. (2002)
K232 y K270	440–445	Kyriakidis and Skarkalis (2000)
Vitamin E derivatives	525	
Chlorophylls	681	

to investigate the spectral data set and to isolate areas, patterns, or latent variables correlated with the information concerned.

Figure 10.17 summarizes the classical steps for building a mathematical model (i.e., a quantitative or discriminant equation). The steps are the pretreatment of data, outlier detection, calibration, and validation procedures including chemical, internal, and external validation.

[AU25] The following sections briefly describe the data treatments and their respective objectives. For a thorough presentation of the ideas in this section, the reader may refer to Tabachnick and Fidell (1983), Williams and Norris (2001), and Martens and Naes (1989).

10.6.1 Pretreatment of Data

The signal obtained from a spectrometer contains information together with random noise. Noise can cause systematic errors in later predictions through the estimated calibration parameters. Thus, reducing noise or, in other words, improving the ratio of signal to noise is still an advantage.

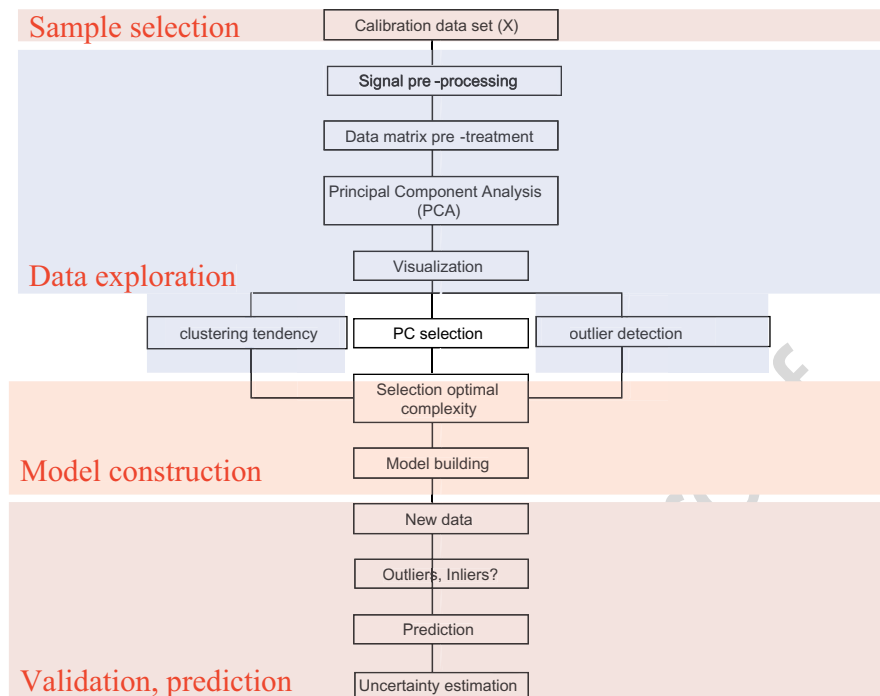


Fig. 10.17 Flow diagram showing principal steps involved in a spectral data treatment

947 Various pretreatments of data are available for different objectives, such as, for
 948 example, to improve the spectral quality (e.g., signal-to-noise ratio), to reduce the
 949 influence of external variation (e.g., variation produced by the sample-handling
 950 method), or to resolve the complexity of overlapping peaks (e.g., the combination
 951 bands or the fingerprint region of MIR spectroscopy). All depend on the objective
 952 sought, the technique investigated, the instrument and sample accessory used, the
 953 sample (neat or solution) studied, the type of mathematical model to be built, or the
 954 researcher's preferences.

955 Various algorithms are available to perform smoothing that basically concern
 956 how to reduce high-frequency ripple noise and, whenever possible, low-frequency
 957 noise. Thus, conceptually speaking, smoothing is simply a filtering process. From
 958 the large panoply of algorithms developed for electronic analog and computer systems
 959 from the 1960s to today, algorithms are available in the smoothing routines of
 960 the software packages developed for IR and Raman spectrometers. These routines
 961 usually contain algorithms such as moving average filters (Rabiner and Gold 1975),
 962 the least-squares polynomial smoothing developed by Savitsky and Golay (1964),
 963 and the classical Fourier smoothing methodology (Williams and Norris 2001;
 964 Martens and Naes 1989), among others. The running mean algorithm simply
 965 replaces the value at each point by the mean of the values in a wavelength (or

wavenumber) interval surrounding it. The interval is centered at the given point, resulting in an odd number of data points per mean (Williams and Norris 2001). The Savitsky–Golay algorithm, the most familiar method of smoothing in analytical chemistry, is an indirect filter that fits the spectrum inside a wavelength (or wavenumber) interval with a polynomial by least-squares method. The parameters are the degree of the polynomial and the number of points to fit (Savitsky and Golay 1964). Fourier analysis makes an orthogonal transformation of the spectrum into a sum of sine and cosine spectral contributions (Aparicio et al. 1977) that allows certain frequencies to be kept (usually low frequencies) and removes those undesired frequencies that do contribute to noise (often the high-frequency ripple). The inverse FT is ultimately used for regenerating the spectrum.

Derivatives allow some compensation for the problems associated with overlapping peaks and baseline variations. Analysts generally use the first and second derivatives. This mathematical treatment calculates the tangent at each point of the raw spectral data. Each inflection point of the raw spectrum corresponds to a relative minimum or maximum of the first derivative spectrum while all maxima and minima on the raw spectrum are zero in the first derivative spectrum. **The same comments can be made with respect to successive odd derivatives, e.g., third, fifth.** The second derivative is advantageous for the resolution of overlapping peaks. Each minimum of the second derivative spectrum corresponds to a maximum of the raw spectrum, and obviously identical comments can be made regarding successive even derivatives (Williams and Norris 2001).

Normalization means changing a group of spectra so that unwanted sources of variability are suppressed. This helps the graphical understanding of the spectra and can reduce the complexity of the subsequent data treatment necessary to develop a calibration from spectroscopic data. The simplest example of this treatment is the subtraction of the spectral value at a single wavelength or wavenumber (the so-called reference wavelength or wavenumber) from all the spectral values; the result is a set of spectra with zero value at the reference wavelength or wavenumber. Normalization by closure is an alternative. This normalization consists in dividing the signal instrument responses at each wavelength or wavenumber by their sum (or mean) in each spectrum. Martens and Naes (1989) suggest this procedure when there is no variable that dominates the total sum of original instrument responses, but always after a graphical inspection of the ratios between some estimated values for independent variables.

Outliers are abnormal, erroneous, or irrelevant observations that can greatly influence mathematical model construction. A number of phenomena such as operator mistakes, noise spikes, instrument drifts, and inconsistent sample-handling position can affect a spectroscopic analysis (Williams and Antoniszyn 1987). Thus, both objects (cases) and variables can behave as outliers, and they are unavoidable in almost all statistical studies. They can only be removed or corrected. During calibration it is important to have them under control as they could decrease the prediction ability of the estimated calibration coefficients. The cross-validation curve can give clues about the presence of outliers in the calibration set, e.g., irregular deviations of the fitted curve of MSE versus the number of PLS factors (Martens and

1011 Naes 1989), although almost all multivariate statistical procedures have algorithms
1012 for outlier detection (Tabachnick and Fidell 1983). Other algorithms are based on
1013 leverage (a Mahalanobis distance that measures the position of independent vari-
1014 ables relative to the rest) and residuals (difference between predicted and observed
1015 values in regression). Leverage is outlier sensitive, and a high leverage observation
1016 in a regression process means that the calibration set contains outliers. A plot of
1017 residuals (residuals against wavelength numbers) gives more than graphical infor-
1018 mation because an observation with large residuals indicates the presence of abnor-
1019 mal information (Cook and Weisberg 1982).

1020 During prediction it is almost compulsory to have methods for detecting abnor-
1021 malities in order to increase the certainty of the predicted results. The detection of
1022 these possibly abnormal observations can be based on data information such as the
1023 residual value and the prediction leverage (Martens and Naes 1989) or more classi-
1024 cal methods based on the Mahalanobis distances (De Maesschalck et al. 2000) and
1025 on potential functions (Jouan-Rimbaud et al. 1999). Robust methods (Geurts et al.
1026 1990) can also be applied such as resampling by the half-means (RHM) or the
1027 smallest half-volume method (SHV) (Egan and Morgan 1998; Pell 2000). However,
1028 most of these multivariate outlier detection techniques are often difficult to under-
1029 stand for nonspecialists and are not an easy matter due to the masking and swamp-
1030 ing effects. The masking effect occurs when one outlier masks a second outlier. In
1031 this case, the second outlier can be considered an outlier only by itself, not in the
1032 presence of the first outlier. In the swamping effect, one outlier swamps a second
1033 observation because the latter can be considered an outlier only in the presence of
1034 the first one (Ben-Gal 2005). Most analytical chemists want to spend as little time
1035 as possible looking at the large variety of diagnostics for outlier detection. In conse-
1036 quence, simple methods are needed. For this reason, complete protocols for outlier
1037 detection have been developed with the maximum information that can be extracted
1038 from the data (Høy et al. 1998; Fernández Pierna et al. 2002). These protocols
1039 include not only the determination of classical measurements as Mahalanobis dis-
1040 tance or the leverage value, but also the calculation of the uncertainty present in the
1041 outputs of the multivariate model, which is calculated as a function of the different
1042 sources of uncertainty present in the model (Fernández Pierna et al. 2003).

1043 After analysis of the internal and external variables that can affect the mathemat-
1044 ical model, the pretreatment of data should finish with a study of the repeatability
1045 and reproducibility of the model. The main element of repeatability is the standard
1046 deviation of a successive collection of spectra of the same sample under the most
1047 realistic experimental conditions. The repeatability study should include not only
1048 all the steps included in the data collection procedure (washing of the sample holder,
1049 sample removal, spectral acquisition), but also a study of the variability observed on
1050 different days. Reproducibility would imply a collaborative study about the com-
1051 parison of spectral results of selected samples by diverse instruments at different
1052 laboratories. The results of the repeatability and reproducibility studies firmly deter-
1053 mine the number of replicates of each case (sample) of the calibration and valida-
1054 tion sets and the regions of the spectra that can be used in calibration.

10.6.2 Mathematical Model Construction

1055

The purpose of IR and Raman instruments is to determine the concentration of chemical variables, such as *trans* content (i.e., quantitative analysis), or the assessment of qualitative issues, such as authenticity or characterization (i.e., qualitative analysis). But to do this, the instrument must be calibrated for converting the IR or Raman optical signal to the desired quantitative or qualitative measurement. A model needs two processes, the calibration, or model design, and the validation, or model verification.

1056
1057
1058
1059
1060
1061
1062

Calibration is usually carried out with chemical parameters (i.e., iodine value) quantified by nonspectroscopic techniques, e.g., chromatography. The dependent variable (e.g., iodine value) is then qualified as a direct measurement, while the independent variable (the spectrum) is described as an indirect measurement. However, it is the spectroscopic technique that responds directly to the problem description. For example, peptide bonds in proteins are directly represented in the spectrum, whereas the so-called direct method Kjeldahl analysis for proteins involves the measurement of total nitrogen, which requires several reaction steps and the application of a conversion factor to amine and protein measurement (Scotter 1997).

1063
1064
1065
1066
1067
1068
1069
1070
1071
1072

10.6.2.1 Calibration in Quantitative Analysis

1073

Calibration means a formula (linear or nonlinear) establishing a relationship between the variation of the spectral data (independent variable) and the chemical reference data (dependent variable). The calibration is in fact a regression process with a strict pretreatment of data and rigorous analysis of the results.

1074
1075
1076
1077

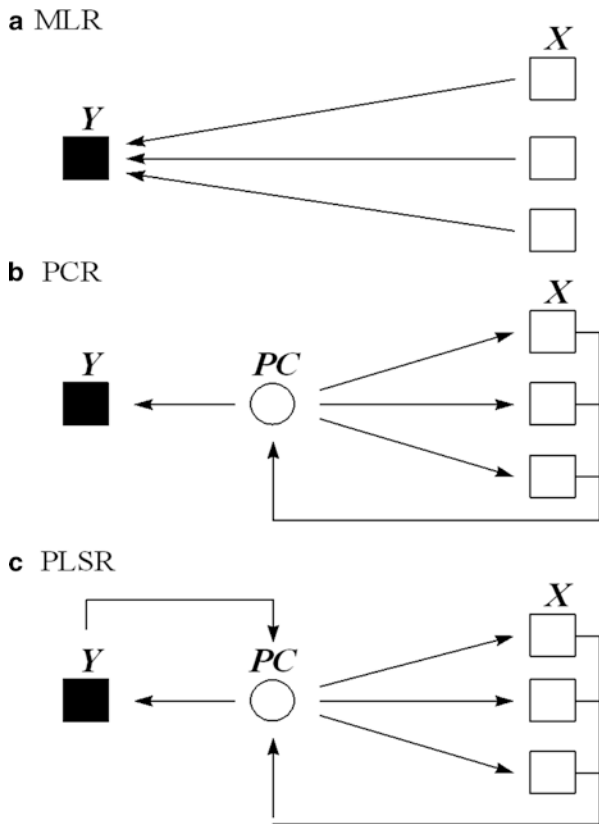
Since two steps are necessary to achieve a mathematical model construction (calibration and validation), two sample sets are necessary, i.e., a set of N samples that would be used to construct the equation (calibration set) and a set of M samples that would allow studying the precision and the reliability of the equation (validation set). The number of samples in the validation set should be at least half of the calibration set. Moreover, the mean and the standard deviation of the two sample sets must be as close as possible, and the validation set must also be a subset of the calibration set covering the whole range of values. To assure these conditions and to have two homogeneous data sets, i.e., which should cover the experimental region uniformly, various methods have been developed and are described in the literature. The most common technique is the duplex method (Snee 1977), which is a modification of the Kennard and Stone technique (Kennard and Stone 1969). In this method, a sequential procedure is applied in order to split the data into two subsets. The method starts by selecting the two points that are furthest from each other and puts them both in a first set (training). Then, the next two points that are furthest from each other are put in a second set (testing), and the procedure is continued by alternately placing pairs of points in the first or second set.

1078
1079
1080
1081
1082
1083
1084
1085
1086
1087
1088
1089
1090
1091
1092
1093
1094

[AU27]

[AU28]

Fig. 10.18 Schematic presentation of (a) multivariate regression analysis (MLR), (b) principal component regression (PCR), and (c) partial least-squares regression (PLSR)



1095 Various calibration (or regression) procedures exist, with multiple linear regression
 1096 (MLR), **polymerase chain reaction** (PCR), and PLS being the most commonly
 1097 used in spectroscopy. Figure 10.18 shows a schematic design of these statistical
 1098 procedures where the matrix Y_{ij} (or \mathbf{y}) represents the values of the j -dependent variables
 1099 (usually chemical analyses) of N ($i = 1 \dots N$) calibration samples, while matrix
 1100 X_{iw} (or \mathbf{X}) represents the values of w -independent variables (spectral wavenumbers or
 1101 wavenumbers) of these N calibration samples. The simple regression equation can
 1102 be written, in matrix convention, $\mathbf{y} = \mathbf{X}\mathbf{b} + \mathbf{f}$, while the objective of the calibration by
 1103 least squares is to minimize the length $\mathbf{f} = \mathbf{y} - \mathbf{X}\mathbf{b}$ whose solution is equal to
 1104 *Estimator*- $\mathbf{b} = (\mathbf{X}'\mathbf{X})^{-1} \mathbf{X}'\mathbf{y}$, where \mathbf{X}' is the transpose matrix \mathbf{X} and \mathbf{X}^{-1} is the
 1105 inverted matrix \mathbf{X} .

[AU29]

1106 The explanation of a dependent variable (e.g., iodine value) by only one wave-
 1107 number is rather difficult, and hence calibration needs to combine more than one
 1108 wavenumber; this is multivariate calibration. Traditional MLR and stepwise multi-
 1109 ple linear regression (SMLR) are expressed as

$$y = b_0 + \sum X_i b_i + \delta,$$

1110

[AU30] where y is the dependent variable, or analytical reference, $X_{i(i=1,n)}$ (the independent variables) are the spectral data (transformed or not) at the respective n wavelengths or n wavenumbers, and b_i ($i = 0, 1, \dots, N$) are the regression coefficients. To achieve higher regression values, the analyst might be tempted to increase the number of spectral data in calibration; however, it is judicious to limit the number according to the sample number. Tabachnick and Fidell (1983) suggest that the number of samples should be ten times the number of independent variables. Anyway the MLR predictor has a deficient performance when there is collinearity in \mathbf{X} , while SMLR gives a better prediction when an F-test is used for selecting variables because this algorithm enables removal of those X_i -variables that are most nonlinear in their response (Tabachnick and Fidell 1983).

Partial least-squares regression (PLSR) was designed to give a plausible solution to those studies where there are many collinear variables and a small calibration set, that is to say, where the number of variables is greater than cases (spectra), although some pitfalls have been described (Defernez et al. 1996). PLSR can be applied for one single y -variable and several y -variables. In general PLSR-1 is more complex than PCR or PLSR-2 than canonical correlation based on simultaneous PCA of \mathbf{X} and \mathbf{Y} matrices. Martens and Naes (1989) state that calibration methods based on PLS regression can give a good understanding of the calibration data and a good approximation of many types of nonlinearities. Other alternative is ridge regression (Pfaffenberger and Dielman 1990), although it has not been widely used in spectroscopy despite the fact that it can be superior to PCR.

One of the most common applications of PCA is in those studies where X_i -variables are expected to be collinear. This is the case with spectral analysis (Cowe et al. 1985a, b), and PCA is able to express the main information in the variables of the raw calibration set by a lower number of variables, so-called principal components (Chap. 12). Once the analyst has decided how many principal components are necessary for retaining the essential information in \mathbf{X} (i.e., applying cross validation), the rest of the process is similar to MLR, although the application of SMLR to PCA is strongly advised (Aparicio et al. 1992). At any rate, the analyst should select the best spectral data instead of the whole spectrum as the latter can contain large amounts of noise or superfluous information.

The described regression procedures assume that the relationship between the independent variables and the dependent variable is linear in nature. However, the nonlinear estimation leaves it up to the analyst to specify the nature of the relationship; for example, you may specify the dependent variable to be a logarithmic function of the independent variables, an exponential function, a function of some complex ratio of independent measures, etc. There are many noncategorical nonlinear estimations such as the quasi-Newton method (O'Neill 1971), piecewise nonlinear regression, Hooke-Jeeves method (Hooke and Jeeves 1961), simplex procedure (Fletcher and Reeves 1964), Hessian method, and others. Where all these other methods fail, the Rosenbrock pattern search method often succeeds. This method rotates the parameter space and aligns one axis with a ridge while all other axes remain orthogonal to this axis. If the loss function is unimodal and has detectable ridges pointing toward the minimum of the function, then this method will proceed

1156 with accuracy toward the minimum of the function. However, if all variables of
1157 interest are categorical in nature, or can be converted into categorical variables, the
1158 correspondence analysis module should also be considered.

1159 It is important to note that sometimes data are nonlinear. Deletion or appropriate
1160 weighting of nonlinear variables at the beginning of an analysis can decrease the
1161 nonlinearity problems. Also, in some cases an appropriate signal preprocessing can
1162 correct for the nonlinearity. These approaches can perhaps give better predictive
1163 ability than linear models with original variables or less complex models for the
1164 same predictive ability; however, alternatively, one may decide to adopt nonlinear
1165 models such as neural networks, support vector machines (SVMs), or local regres-
1166 sion approaches (De Maesschalck et al. 1999).

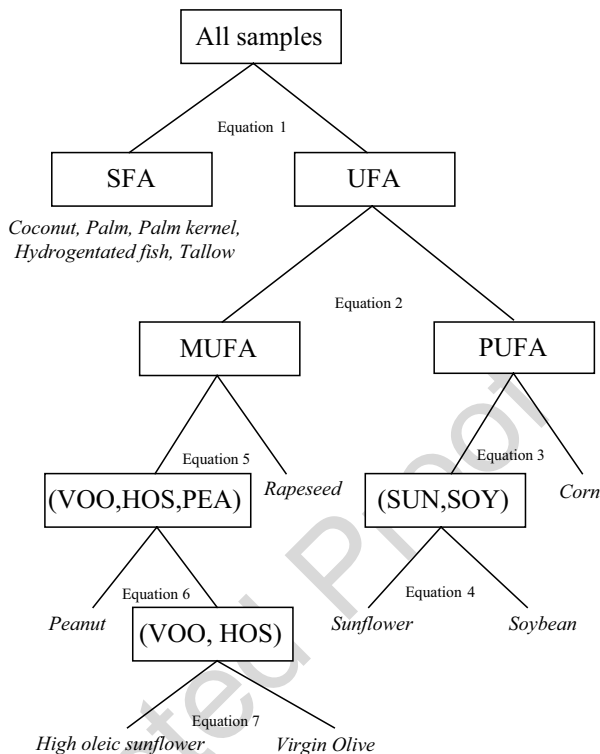
1167 10.6.2.2 Qualitative Analysis: Classification Protocols

1168 To construct a mathematical model for olive oil characterization or authentication,
1169 it is important to establish an intelligible, reproducible, valid, and predictive
1170 approach. Unfortunately, few authors propose a complete procedure to extract and
1171 use the information contained in IR or Raman spectra. The following sections are
1172 based on the results obtained with two protocols (Lai et al. 1994).

1173 The first step of these two approaches is identical and concerns the division of
1174 the sample set into two subsets. As mentioned previously, the first subset (calibra-
1175 tion set) is used to construct the discrimination equation, while the second subset
1176 (validation set) permits the validation of the established model. The sample set stud-
1177 ied must include all possible combinations of variables and the variation in all direc-
1178 tions should be as large as possible but limited to the direction of interest (Naes and
1179 Isakson 1989).

1180 In the procedure suggested by Lai et al. (1994), PCA is used because it consti-
1181 tutes an efficient data reduction method. As mentioned previously, a spectrum con-
1182 tains several hundred variables. But a multivariate statistical analysis requires that
1183 the case (sample) number exceed the variable number, and as a consequence, a
1184 reduction in the spectral variable number is necessary. Furthermore, the PCA proce-
1185 dure allows the removal of the apparent redundancy of the variables by transform-
1186 ing the original data into a set of principal component scores. When this is done, a
1187 rearrangement of the data takes place and the first few PC scores are sufficient to
1188 describe the information contained in the original variables. This procedure allows
1189 for data set simplification and the visualization of relationships within the data.
1190 After applying PCA, Lai et al. (1994) used discriminant analysis to construct a
1191 mathematical model on the basis of the scores. The squared Mahalanobis distances
1192 (SMDs) are used to classify each case (sample) inside the predetermined groups.
1193 Later, the SMDs from the established group means are calculated for each valida-
1194 tion spectrum's PC scores and the new samples will be assigned to the nearest group
1195 mean. The percentage of correct classifications corresponds to the samples assigned
1196 to the correct group (i.e., species).

Fig. 10.19 Discrimination tree constructed using near-infrared and Raman spectral data. Legend: *SFA* samples rich in saturated fatty acids, *UFA* samples rich in unsaturated fatty acids, *MUFA* samples rich in monounsaturated fatty acids, *PUFA* samples rich in polyunsaturated fatty acids, *VOO* virgin olive oil, *HOS* high oleic sunflower, *PEA* peanut, *SUN* sunflower, *SOY* soybean



The approach presented by Aparicio and Baeten (1998) uses stepwise linear discriminant analysis (SLDA) to select frequencies and construct the mathematical models. SLDA is first applied to each part of the spectrum in such a way that the more relevant frequencies from each region are selected. After that, the SLDA procedure is applied to all the preselected variables and the discriminating equations are established on the basis of Mahalanobis distance and F-test (Tabachnick and Fidell 1983). The ellipses of the 95 % confidence region are calculated for each predetermined group during the calibration step (Aparicio and Baeten 1997). These ellipses allow an interpretation beyond the simple location of a validation sample and the calculation of the percentage of samples correctly classified during the validation procedure (Aparicio and Morales 1995). An alternative to these procedures could be to apply the Fisher test for removing variables without precise information and then apply PCA on the selected variables. The model can be used in an arborescent structure for distinguishing different types of fats and oils (Fig. 10.19).

Also, classical chemometric methods such as partial least squares discriminant analysis (PLSDA) (Martens and Naes 1989), and artificial neural networks (ANNs) (Despagne and Massart 1998) are well-known and proven techniques for both qualitative and quantitative analysis of multivariate data. In the case of qualitative analysis, the SVM technique (Vapnik 2000) has been recently proposed and widely used in the literature (Burgos 1998; Belousov et al. 2002; Fernández Pierna et al. 2004).

1217 The choice of SVM as classification method is justified by the great performance of
1218 these methods in all studies, which is mainly due to the uniqueness of the SVM
1219 solution for the problems of pattern recognition.

1220 **10.6.3 Validation Procedures**

1221 Analysts should pay attention to the validation procedures, which include the chem-
1222 ical, internal, and external validations (Fig. 10.17). Chemical validation is the inter-
1223 pretation and the elucidation (band assignment) of the frequencies used in the
1224 mathematical model. All selected spectral data (frequencies) should have a chemi-
1225 cal or physical explanation in order to avoid regressions obtained by chance. To do
1226 this step successfully, the study of the spectral features (position and intensity of the
1227 bands) of pure chemical compounds and the correlation at each frequency between
1228 the intensities and chemical properties (e.g., determined by gas chromatography) is
1229 necessary.

1230 Internal and external validations consist in the study of the efficiency and power
1231 of the mathematical models constructed. Internal validation is done with the sam-
1232 ples involved in the construction of the equation (calibration step). Cross validation
1233 is a particular internal validation method (Martens and Naes 1989), although there
1234 are others such as leverage correction or Mallows C_p statistic (Chap. 10). An exter-
1235 nal validation is made by the observation of the quantification (quantitative analy-
1236 sis) or the classification (qualitative analysis) of new samples not used in the
1237 calibration procedure. The number and characteristics of these samples have been
1238 clearly established (Aparicio et al. 1992).

1239 In order to perform a correct validation and to indicate the performance of the
1240 results, different standard expressions taken from basic statistics are applied.
1241 However, multivariate models are inherently complex, and as a result, theoretical
1242 advances with respect to the corresponding error analysis are relatively slow. For
1243 this reason, developing approximate expressions for sample-specific standard error
1244 of prediction when applying a multivariate model, mainly PLS, has received consid-
1245 erable attention in the chemometric-related literature in recent years (Faber 2000;
1246 Faber and Bro 2002). This calculation of uncertainty consists in the study of the
1247 uncertainty present in the outputs of the model. In most cases, this uncertainty is
1248 calculated as a function of the various sources of uncertainty present in the model
1249 (Fernández Pierna et al. 2003).

1250 **10.7 Potential of Infrared and Raman Spectroscopy**

1251 The potential offered by NIR, MIR, and Raman spectroscopy in the determination of
1252 various chemical compounds and chemical indices has been described, with more or
1253 less success, by various authors (Williams and Norris 1987; van de Voort 1994;

Li-Chan 1996; Guillén and Cabo 1997). The following section briefly describes the methods used with olive oil, whereas their application in characterization is described in Chap. 12.

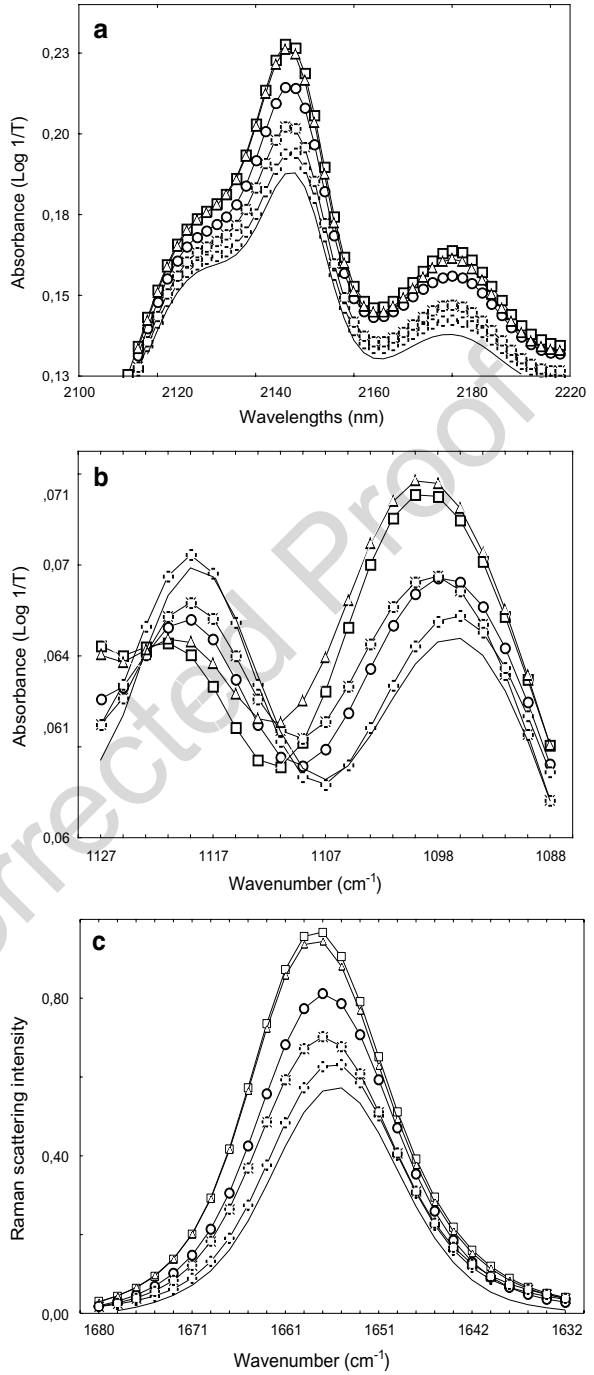
10.7.1 Determination of Unsaturation Degree: Iodine Value

As was mentioned earlier, NIR, MIR, and Raman spectrum profiles are strongly influenced by the content and type of unsaturated groups. Figure 10.20 presents a spectral region of various edible oils and fats for each technique investigated. The regions shown are, respectively, the region 2,100–2,200 nm (=C-H vibration) of NIR spectra, the region 1,130–1,080 cm^{-1} (C-C and C-O-C vibration) of MIR spectra, and the region 1,680–1,650 cm^{-1} (C=C vibration) of Raman spectra.

Fenton and Crisler (1959) published a study showing the potential of NIR spectroscopy. They developed, using a series of chemical products, a rapid and reliable technique for the determination of the iodine value. The calibration equation was constructed with the information contained in the region 2,100–2,200 nm of the NIR spectrum. Some years earlier, Sinclair et al. (1952) had described the linear relationship between the number of *cis* double bonds of unsaturated fatty acid methyl esters and the ratio between the absorbance at 2,920 cm^{-1} ($>\text{CH}_2$ vibration) and the difference between the absorbances at 2,920 and 3,020 cm^{-1} (=C-H vibration). This study was later confirmed by the results achieved by other authors who proposed MIR spectroscopy as a technique to determine the degree of unsaturation (Chapman 1965). Later, Arnold and Hartung (1971), using the ratio of absorbances at 3,030 cm^{-1} (=C-H vibration) and 2,857 cm^{-1} ($>\text{CH}_2$ vibration), showed the potential of a MIR instrument equipped with a transmission cell for iodine value determinations in fats and oils. Using the absorbance of wavenumbers from the same region (3,010 and 2,854 cm^{-1}), Afran and Newbery (1991) demonstrated the potential of an FT-MIR instrument coupled with an ATR accessory. The absorption intensities at 3,007 cm^{-1} (=C-H vibration) (Muniategui et al. 1992) and at 1,658 cm^{-1} (C=C vibration) (Bernard and Sims 1980) were also used to determine the total degree of unsaturation.

A FT-MIR/ATR instrument, together with a PLS procedure, was used by van de Voort et al. (1992) for determining the iodine value using TAGs as dependent variables. Spectral information from regions 3,200–2,600 cm^{-1} and 1,600–1,000 cm^{-1} was successfully used. Bailey and Horvat (1972) showed the high correlation between the iodine value and the ratio of the scattering intensities in the regions 1,691–1,626 cm^{-1} (C=C vibration) and 1,478–1,420 cm^{-1} ($>\text{CH}_2$ vibration) using Raman spectroscopy. Later, a Raman spectrometer equipped with a NIR excitation and interferometry technology was used by Sadeghi-Jorabchi et al. (1990) to study the possibilities offered by the new generation of such instruments in the determination of iodine value of oils and margarines. The quantitative program designed in this study used information from the scattering bands centered at 1,656 cm^{-1} (=C-H

Fig. 10.20 Spectral regions of (a) near-infrared, (b) FT-mid-infrared, and (c) FT-Raman spectra of different edible oils



vibration) and at $1,444\text{ cm}^{-1}$. The peaks in the vicinity of $3,010\text{ cm}^{-1}$ (=C-H stretching vibration) and $1,270\text{ cm}^{-1}$ (=C-H bending vibration) also showed a high correlation with the iodine value (Sadeghi-Jorabchi 1991; Baeten et al. 1998).

10.7.2 Determination of Trans and Cis Content

Infrared methods for determining the *trans* isomer content of oils and fats are standardized (IUPAC 1992; AOCS 1988). These methods are based on the absorption band at 967 cm^{-1} (*trans* CH=CH vibration). However, Lanser and Emken (1988), using the peak area of the *trans* absorbance band at 966 cm^{-1} , estimated the *trans* unsaturation, which agreed with the results obtained by gas chromatography. Belton et al. (1988) used FT-MIR combined with ATR to develop a procedure for the estimation of isolated *trans* double bonds in oils and fats. Sleeter and Matlock (1989) developed a FT-MIR procedure for measuring the *trans* content of oils in a $100\text{-}\mu\text{m}$ KBr cell. Ulberth and Haider (1992) used *trans*-free methylated soybean oil mixed with methyl elaidate in combination with a FT-MIR spectral subtraction technique and PLS to assess low concentrations of isolated *trans* double bonds in hydrogenated fats such as margarine and shortenings. Then, van de Voort et al. (1995) designed a generalized, industrial sample-holder accessory for handling both fats and oils. It was incorporated into a FT-MIR spectrometer, and a method using PLS calibration was developed to determine the *cis* and *trans* contents of neat samples. Mossoba et al. (1996) also used attenuated total reflection spectroscopy to calculate the total *trans* content of hydrogenated oils by the information of the spectral region between 990 and 945 cm^{-1} .

[AU32] Using Raman spectroscopy, Bailey and Horvat (1972) also determined the *cis/trans* isomer content of edible vegetable oils by measuring the intensities of C=C stretching fundamentals near $1,657$ and $1,670\text{ cm}^{-1}$ that are associated with *cis* and *trans* configurations, respectively. As seen earlier, the use of FT-Raman spectroscopy has proved to be successful in the determination of total unsaturation of oils and margarines (Sadeghi-Jorabchi et al. 1990). Furthermore, Sadeghi-Jorabchi et al. (1991) have also used the FT-Raman scattering information from bands centered near $1,670$, $1,656$, and $1,444\text{ cm}^{-1}$ to estimate various levels of *cis* and *trans* isomers mixtures. A similar approach was used by Ozaki et al. (1992) to estimate the level of unsaturation of a wide range of fat-containing foodstuffs.

10.7.3 Determination of Saponification Number, Solid Fat Index, and Free Fatty Acids

Using the information obtained from a FT-MIR spectrometer equipped with an ATR accessory and the PLS methodology, van de Voort et al. (1992) proposed a method to determine the saponification number. They used the information contained in two

1331 MIR regions: 3,200–2,600 cm^{-1} and 1,850–1,000 cm^{-1} . Van de Voort et al. (1996)
1332 also showed the potential of MIR spectroscopy in the determination of the solid fat
1333 index. The calibration was done with selected parts of the spectrum: 3,015–
1334 3,005 cm^{-1} , 3,000–2,850 cm^{-1} , 1,750–1,740 cm^{-1} , 1,550–1,050 cm^{-1} , 980–960 cm^{-1} ,
1335 and 750–730 cm^{-1} by a FT-MIR spectrometer equipped with a flow transmission
1336 cell and PLS. Lanser et al. (1991) used peaks near 1,745 and 1,711 cm^{-1} to construct
1337 a model allowing the determination of the free fatty acid content in crude oils. The
1338 C=O carbonyl group of esters is present near 1,746 cm^{-1} , while the carboxylic
1339 group of free fatty acids has its characteristic peak at 1,711 cm^{-1} . Later, an FT-MIR
1340 instrument and ATR accessory were successfully used to determine the free fatty
1341 acid content in oils and fats (Ismail et al. 1993).

1342 **10.7.4 Monitoring the Oxidative Process, Measuring** 1343 **the Peroxide and Anisidine Values**

1344 The potential of FT-MIR instruments for the study of the complex changes that take
1345 place in a sample involved in an oxidation process has also been investigated (van
1346 de Voort et al. 1994a). The authors used oils oxidized under various conditions and
1347 recorded their MIR spectral changes. They identified the most noteworthy bands
1348 associated with common oxidation end products such as, for example, hexanal,
1349 decadienal, (E)-butyl hydroxide, demonstrating the usefulness of FT-MIR spectroscopy
1350 to detect oxidative changes.

1351 A method based on FT-MIR spectroscopy was also proposed for the simultane-
1352 ous monitoring of aldehyde formation and the determination of the anisidine value
1353 in thermally stressed oils (Dubois et al. 1996). The authors added aldehydes to an
1354 oil sample and thus built a calibration model by PLS.

[AU33]

1355 **10.8 Potential of Fluorescence Spectroscopy**

1356 Fluorescence spectroscopy is a rapid analytical technique with high sensitivity to
1357 determine the overall presence of series of compounds. The use of fluorescence to
1358 analyze olive oils was first proposed in 1925 by Frehse, who studied the possibility
1359 of detecting the presence of refined olive oil in virgin olive oil by examining the oils
1360 under a quartz lamp with a Wood filter; another early work showed good prospects
1361 for characterization of edible oils through fluorimetry techniques (Wolfbeis and
1362 Leiner 1984). However, this highly sensitive technique has been largely ignored for
1363 the characterization of edible oils. Only recently has progress been achieved in
1364 spectrofluorometers and several fluorescence techniques that have been introduced
1365 to facilitate the analysis of complex food. Thus, fluorescence spectroscopy has con-
1366 siderable potential to characterize virgin olive oils because of the large variety of
1367 fluorescent compounds (chlorophylls, pheophytins, tocopherols, vitamin E, and

oxidized compounds) present in them (Sikorska et al. 2004; Guimet et al. 2004; Galano et al. 2003). On the other hand, there are remarkable differences between the fluorescence spectra of virgin olive oil and the other edible oils (Sikorska et al. 2005), which encourages the use of this technique for authentication purposes. The various categories of virgin olive oil also show particular emission spectra (Nicoletti 1990).

Some progress have been made in the development of new methods to detect adulteration, such as fraudulent mixtures of olive oil with hazelnut oil (Sayago et al. 2007), or to detect the oxidation degree of oils (Poulli et al. 2009a, b). The application of more advanced methods as EEFS and SFS makes the interpretation of the spectra more easy and informative than conventional spectroscopy.

Many fluorescent compounds present in virgin olive oil are involved in oxidation (e.g., phenols and vitamin E), and they evolve during different culinary practices such as frying. For that reason, fluorescence spectroscopy has recently been applied to evaluate the quality of thermoxidized oils (Tena et al. 2009, 2012). Other applications include the study of oil deterioration during long-term storage (Sikorska et al. 2008).

10.9 Conclusions 1383

The previous sections have shown the potential of IR, Raman, and fluorescence spectroscopic techniques in oil analysis. NIR, MIR, and Raman spectra mainly contain information about unsaturated compounds. NIR spectroscopy can be used to determine the total level of unsaturation and the content of *cis* isomers. Excitation and emission fluorescence spectra provide information about the minor compounds present in olive oil. The low cost and the possibility of coupling the NIR spectrometer to classical optical fibers provide a designed technique for implementation in continuous processes. MIR spectroscopy is classically used to determine the content of *trans* isomers, while information about *cis* isomers exists but is more limited. A MIR spectrometer seems to be an appropriate instrument for analytical laboratories. In fact, recent studies have demonstrated the great potential of MIR spectroscopy in the determination of classic chemical values and oil indices. The potential of this technique in the monitoring of oxidative processes is an additional advantage.

New developments in the instrumentation of Raman spectroscopy have promoted its importance for oil analysis. Raman spectra mainly contain information about *cis* and *trans* isomers. Due to the chemical origin of the bands, the information contained in the spectrum may be used to develop techniques for the determination of the total content of unsaturation, the type of unsaturation, and *cis/trans* isomer composition. In addition, a Raman spectrometer does not need a special sample-handling accessory and may be coupled to low-cost optical fibers.

In addition to the possibilities offered in quantitative analysis and in monitoring oxidative processes, IR and Raman spectroscopy show interesting perspectives in the characterization and adulteration detection of virgin olive oil. To compare the potential of NIR, MIR, and Raman spectroscopy in this domain, the spectra of 64 edible oils from seven varieties (corn, soybean, rapeseed, peanut, sunflower, high

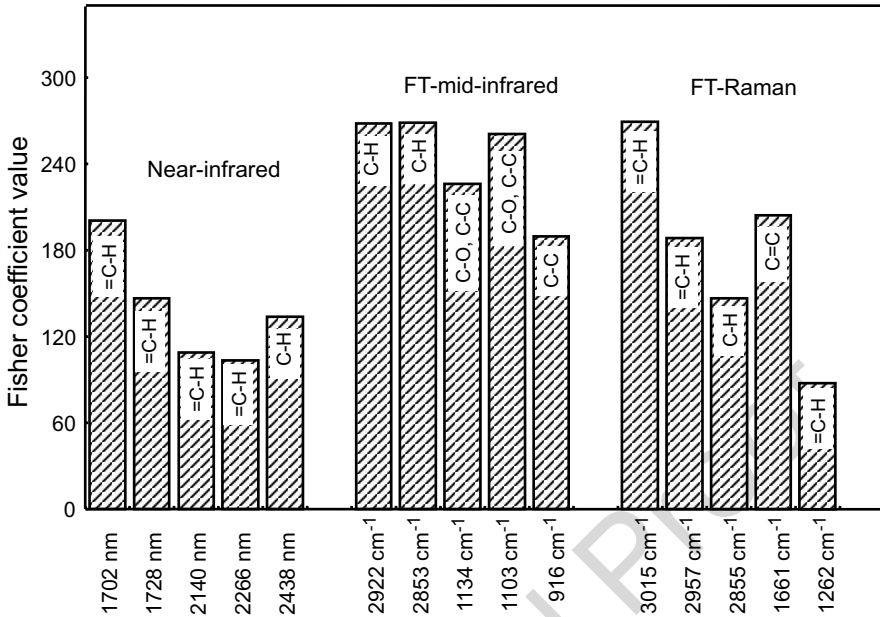


Fig. 10.21 The five most discriminant wavelengths (or wavenumbers) resulting from the study of near-infrared, FT-mid-infrared, and FT-Raman spectra of seven edible oil sources (corn, high oleic sunflower, peanut, rapeseed, soybean, sunflower, and virgin olive oils)

1409 oleic sunflower, and virgin olive oils) were collected (Aparicio and Baeten 1998).
 1410 The Fischer coefficient was used to underline the wavelengths and the wavenum-
 1411 bers having the highest power of varietal discrimination. Figure 10.21 displays, for
 1412 each technique studied, the five most discriminant wavelengths or wavenumbers.
 1413 NIR spectral data present Fischer coefficients lower than the data obtained in MIR
 1414 and Raman spectroscopy. Four wavelengths underlined in NIR spectroscopy corre-
 1415 spond to the C-H vibration of unsaturated groups. On the other hand, the wavenum-
 1416 bers extracted in MIR spectroscopy are characteristic of the C-H and C-C vibrations
 1417 of the carbon skeleton and of the C-O of the ester groups. As in NIR spectroscopy,
 1418 part of the Raman spectral data selected corresponds to the C-H vibration of unsatu-
 1419 rated groups. The other wavenumbers are characteristics of C-H and C=C vibra-
 1420 tions. Figure 10.10 clearly shows complementarity between vibrational spectroscopy
 1421 (i.e., NIR and MIR spectroscopic techniques). This information can benefit from
 1422 fluorescence spectroscopy, particularly in oxidation studies. Fluorescence spectro-
 1423 scopy is very versatile because it makes spectra acquisition possible in different
 1424 modes (EEFS, SFS). These different modes provide several alternatives for a better
 1425 interpretation of the spectra collected with conventional fluorescence spectroscopy
 1426 to establish definitive and nonspeculative chemical assignments of the spectral
 1427 bands like those in MIR, NIR, and Raman spectra.

[AU34] **References**

1428

[AU35]

- Abbas O, Fernández Pierna JA, Codony R, von Holst C, Baeten V (2009) Assessment of the discrimination of animal fat by FT-Raman spectroscopy. *J Mol Struct* 924–926:294–300 1429
1430
- Afran A, Newbery JE (1991) Analysis of the degree of unsaturation in edible oils by Fourier transform-infrared/attenuated total reflectance spectroscopy. *Spectrosc-Int J* 3:39–42 1431
1432
- Ahro M, Hakala M, Kauppinen J, Kallio H (2002) Headspace FT-IR analysis of rapeseed oil oxidation. *Appl Spectrosc* 56:217–222 1433
1434
- American Oil Chemists Society (AOCS) (1988) Official methods and recommended practices of the American Oil Chemist's Society, method Cd 14–61. AOCS Press, Champaign 1435
1436
- Aparicio R, Baeten V (1997) Possibilities offered by infrared and Raman spectroscopic techniques in virgin olive oil authentication. *Olivae* 69:38–43 1437
1438
- Aparicio R, Baeten V (1998) Authentication of olive oil by FT-Raman. *OCL* 5:14–16 1439
- Aparicio R, Morales MT (1995) Sensory wheels: a statistical technique for comparing QDA panels – application to virgin olive oil. *J Sci Food Agric* 67:247–257 1440
1441
- Aparicio R, Montañó J, Rodríguez-Izquierdo G (1977) Reactive power meter for nonsinusoidal systems. *IEEE Trans Instru Meas* 26:258–260 1442
1443
- Aparicio R, Gutiérrez F, Rodríguez-Morales J (1992) Relationship between flavour descriptors and overall grading of analytical panels for virgin olive oil. *J Sci Food Agric* 58:555–562 1444
1445
- Arnold RG, Hartung TE (1971) Infrared spectroscopy determination of degree of unsaturation of fats and oils. *J Food Sci* 36:166–168 1446
1447
- Baeten V, Meurens M, Morales MT, Aparicio R (1996) Detection of virgin olive oil adulteration by Fourier transform Raman spectroscopy. *J Agric Food Chem* 44:2225–2230 1448
1449
- Baeten V, Hourant P, Morales MT, Aparicio R (1998) Oil and fat classification by FT-Raman spectroscopy. *J Agric Food Chem* 46:2638–2646 1450
1451
- Baeten V, Dardenne P, Aparicio R (2001) Interpretation of Fourier transform Raman spectra of the unsaponifiable matter in a selection of edible oils. *J Agric Food Chem* 49:5098–5107 1452
1453
- Baeten V, Fernández Pierna JA, Dardenne P, Meurens M, García González DL et al (2005) Detection of the presence of hazelnut oil in olive oil by FT-Raman and FT-MIR spectroscopy. *J Agric Food Chem* 53:6201–6206 1454
1455
1456
- Bailey GF, Horvat RJ (1972) Raman spectroscopic analysis of the cis/trans isomer composition of edible vegetable oils. *J Am Oil Chem Soc* 49:494–498 1457
1458
- Banwell CN (1994) Fundamentals of molecular spectroscopy. McGraw-Hill, London 1459
- Baranska H, Labudzinska A, Terpinski J (1987) Laser Raman spectrometry: analytical applications. Ellis Horwood, Chichester 1460
1461
- Barrow GM (1973) Physical chemistry. McGraw-Hill, New York 1462
- Bellon-Maurel V, Vigneau JL, Sévila F (1994) Infrared and near-infrared technology for the food industry and agricultural uses: on-line applications. *Food Control* 5:21–27 1463
1464
- Belousov AI, Verzakov SA, von Frese JJ (2002) Applicational aspects of support vector machines. *J Chemometr* 16:482–489 1465
1466
- Belton PS, Wilson RH, Sadeghi-Jorabchi H, Peers KE (1988) A rapid method for the determination of isolated trans double bonds in oils and fats using Fourier transform infrared spectroscopy combined with attenuated total reflectance. *Lebensm Wiss Technol* 21:153–157 1467
1469
- Ben-Gal I (2005) Outlier detection. In: Maimon O, Rockach L (eds) *Data mining and knowledge discovery handbook: a complete guide for practitioners and researchers*. Kluwer Academic Publishers, New York, pp 131–146 1470
1471
1472
- Bernard JL, Sims LG (1980) IR spectroscopy for determination of total unsaturation. *Res Dev* 8:81–83 1473
1474
- Blanco M, Villarroya I (2002) NIR spectroscopy: a rapid-response analytical tool. *Trends Anal Chem* 21:240–250 1475
1476
- Burges CJC (1998) A tutorial on support vector machines for pattern recognition. *Data Min Knowl Disc* 2:121–167 1477
1478

- 1479 Cayuela JA, Pérez Camino MC (2010) Prediction of quality of intact olives by near infrared
1480 spectroscopy. *Eur J Lipid Sci Technol* 112:1209–1217
- 1481 Cayuela JA, García JM, Caliani N (2009) Predicción NIR de la humedad del fruto, acidez libre y
1482 contenido de aceite en aceitunas intactas. *Grasas Aceites* 60:194–202
- 1483 Chapman D (1965) Infrared spectroscopy of lipids. *J Am Oil Chem Soc* 42:353–371
- 1484 Chase B (1987) Fourier transform Raman spectroscopy. *Anal Chem* 59:881A–889A
- 1485 Cook RD, Weisberg S (1982) Residuals and influence in regression. Chapman and Hall, London
- 1486 Cowe IA, McNicol JW, Cuthbertson DC (1985a) A designed experiment for the examination of
1487 techniques used in the analysis of near infrared spectra. Part 1. Analysis of spectral structure.
1488 *Analyst* 110:1227–1232
- 1489 Cowe IA, McNicol JW, Cuthbertson DC (1985b) A designed experiment for the examination of
1490 techniques used in the analysis of near infrared spectra. Part 2. Derivation and testing of
1491 regression models. *Analyst* 110:1233–1240
- 1492 De Maesschalck R, Estienne F, Verdú-Andrés J, Candolfi A, Centner V et al (1999) The develop-
1493 ment of calibration models for spectroscopic data using principal component analysis. *Internet*
1494 *J Chem* 2:19
- 1495 De Maesschalck R, Jouan-Rimbaud D, Massart DL (2000) The Mahalanobis distance. *Chemometr*
1496 *Intell Lab* 50:1–18
- 1497 Despagne F, Massart DL (1998) Neural networks in multivariate calibration. *Analyst*
1498 123:157R–178R
- 1499 Diem M (1993) Introduction to modern vibrational spectroscopy. Wiley, New York
- 1500 Dubois J, van de Voort FR, Sedman J, Ismail AA, Ramaswamy HR (1996) Quantitative Fourier
1501 transform infrared analysis for anisidine value and aldehydes in thermally stressed oils. *J Am*
1502 *Oil Chem Soc* 73:787–794
- 1503 Dupuy N, Le Dréau Y, Ollivier D, Artaud J, Pinatel C, Kister J (2005) Origin of french virgin olive
1504 oil registered designation of origins predicted by chemometric analysis of synchronous
1505 excitation-emission fluorescence spectra. *J Agric Food Chem* 53:9361–9368
- 1506 Egan WJ, Morgan SL (1998) Outlier detection in multivariate analytical chemical data. *Anal Chem*
1507 70:2372–2379
- 1508 Faber NM (2000) Response to comments on construction of confidence intervals in connection
1509 with partial least squares. *J Chemometr* 14:363–369
- 1510 Faber NM, Bro R (2002) Standard error of prediction for multiway PLS – 1. Background and a
1511 simulation study. *Chemometr Intell Lab* 61:133–149
- 1512 Fayolle PH, Picque D, Corrieu G (2000) On-line monitoring of fermentation processes by a new
1513 remote dispersive middle-infrared spectrometer. *Food Control* 11:291–296
- 1514 Fenton AJ, Crisler RO (1959) Determination of cis unsaturation in oils by near-infrared spectroscopy. *J Am Oil Chem Soc* 36:620–623
- 1515 Fernández Pierna JA, Wahl F, de Noord OE, Massart DL (2002) Methods for outlier detection in
1516 prediction. *Chemometr Intell Lab* 63:27–39
- 1517 Fernández Pierna JA, Jin L, Wahl F, Faber NM, Massart DL (2003) Estimation of partial least
1518 squares regression (PLSR) prediction uncertainty when the reference values carry a sizeable
1519 measurement error. *Chemometr Intell Lab* 65:281–291
- 1520 Fernández Pierna JA, Baeten V, Michotte Renier A, Cogdill RP, Dardenne P (2004) Combination
1521 of support vector machines (SVM) and near infrared (NIR) imaging spectroscopy for the detec-
1522 tion of meat and bone meat (MBM) in compound feeds. *J Chemometr* 18:341–349
- 1523 Fletcher R, Reeves M (1964) Function minimization by conjugate gradients. *Comput J* 7:
1524 149–154
- 1525 Galano T, Durán I, Correa CA, Roldán B, Rodríguez MI (2003) Simultaneous fluorometric deter-
1526 mination of chlorophylls a and b and pheophytins a and b in olive oil by partial least squares
1527 calibration. *J Agric Food Chem* 51:6934–6940
- 1528 Galeano T, Durán I, Correa CA, Roldán B, Rodríguez MI (2003) Simultaneous fluorometric deter-
1529 mination of chlorophylls a and b and pheophytins a and b in olive oil by partial least squares
1530 calibration. *J Agric Food Chem* 51:6934–6940
- 1531

Gallardo-González L, Osorio-Bueno E, Sánchez-Casas J (2005) Application of near infrared spectroscopy (NIRS) for the real-time determination of moisture and fat contents in olive pastes and wastes of oil extraction. <i>Alimentación, Equipos y Tecnología</i> 24:85–89	1532 1533 1534
García-Gonzalez DL, van de Voort FR (2009) A novel wire mesh “cell” for studying lipid oxidative processes by fourier transform infrared spectroscopy. <i>Appl Spectrosc</i> 63:518–527	1535 1536
Gerrard DL, Birnie J (1992) Raman spectroscopy. <i>Anal Chem</i> 64:502R–513R	1537
Geurts MD, Rinne HJ, Lawrence SH (1990) Alternative methods of dealing with outliers in forecasting sales with regression-based methods. In: Lawrence KD, Arthur JL (eds) <i>Robust regression: analysis and application</i> . Marcel Dekker, New York, pp 225–239	1538 1539 1540
Giungato P, Aveni M, Rana R, Notarnicola L (2004) Modifications induced by extra virgin olive oil frying processes. <i>Ind Aliment-Italy</i> 43:369–375	1541 1542
Goddu RF (1957) Determination of unsaturation by near-infrared spectrophotometry. <i>Anal Chem</i> 29:1790–1794	1543 1544
Gonzaga FB, Pasquini C (2006) A new method for determination of the oxidative stability of edible oils at frying temperatures using near infrared emission spectroscopy. <i>Anal Chim Acta</i> 570:129–135	1545 1546 1547
Grasselli JG, Bulkin BJ (1991) <i>Analytical Raman spectroscopy</i> . Wiley, New York	1548
Guillén MD, Cabo N (1997) Infrared spectroscopy in the study of edible oils and fats. <i>J Sci Food Agric</i> 75:1–11	1549 1550
Guimet F, Ferré J, Boqué R, Rius FX (2004) Application of unfold principal component analysis and parallel factor analysis to the exploratory analysis of olive oils by means of excitation-emission matrix fluorescence spectroscopy. <i>Anal Chim Acta</i> 515:75–85	1551 1552 1553
Harrick N (1967) <i>Internal reflection spectroscopy</i> . Wiley, New York	1554
Hendra PJ (1997) Fourier transform Raman spectroscopy in pharmaceutical analysis and research. <i>Int Lab</i> 5:13A–13I	1555 1556
Hermoso M, Uceda M, García-Ortiz A, Jiménez A, Beltrán G (1999) Preliminary results of NIR “on line” measure of oil content and humidity in olive cakes from the two phases decanter. <i>Acta Horticulturae</i> 474:717–719	1557 1558 1559
Herzberg G (1945) <i>Molecular spectra and molecular structure. II. Infrared and Raman spectra of polyatomic molecules</i> . Van Nostrand Reinhold, New York	1560 1561
Hirschfeld T, Chase B (1986) FT-Raman spectroscopy: development and justification. <i>Appl Spectrosc</i> 3:133–141	1562 1563
Holman RT, Edmondson PR (1956) Near infrared spectra of fatty acids and some related substances. <i>Anal Chem</i> 28:1533–1538	1564 1565
Hooke R, Jeeves FA (1961) Direct search solution of numerical and statistical problems. <i>J Assoc Comput Mach</i> 8:212–229	1566 1567
Hourant P (1995) <i>Contrôle de qualité des matières grasses alimentaires par spectroscopie infrarouge</i> . Catholic University of Louvain (UCL), Louvain-la-Neuve	1568 1569
Hourant P, Baeten V, Morales MT, Meurens M, Aparicio R (2000) Oil and fat classification by selected bands of near-infrared spectroscopy. <i>Appl Spectrosc</i> 54:1168–1174	1570 1571
Høy M, Steen K, Martens H (1998) Review of partial least squares regression prediction error in Unscrambler. <i>Chemometr Intell Lab</i> 44:123–133	1572 1573
Huang H, Yu H, Xu H, Ying Y (2008) Near infrared spectroscopy for on/in-line monitoring of quality in foods and beverages: a review. <i>J Food Eng</i> 87:303–313	1574 1575
International Union Pure and Applied Chemistry (IUPAC) (1992) Determination of content of isolated <i>trans</i> -unsaturated compounds by infrared spectrophotometry. In: Dieffenbacher A, Pocklington WD (eds) <i>Standards methods for the analysis of oils, fats and derivatives</i> , 7th edn. Blackwell Scientific Publication, Oxford, pp 99–102, Method 2.207	1576 1577 1578 1579
Ismail AA, van de Voort FR, Emo G, Sedman J (1993) Rapid quantitative determination of free fatty acids in fats and oils by Fourier transform infrared spectroscopy. <i>J Am Oil Chem Soc</i> 70:335–341	1580 1581 1582
Ismail AA, Cocciardi RA, Alvarez P, Sedman J (2006) Infrared and Raman spectroscopy in food science. In: Hui YH (ed) <i>Handbook of food science, technology and engineering</i> . CRC Press, Boca Raton, pp 44.1–44.19	1583 1584 1585

- 1586 Jiménez-Márquez A, Molina-Díaz A, Pascual-Reguera MI (2005) Using optical NIR sensor for
1587 on-line virgin olive oils characterization. *Sensors Actuat B* 107:64–68
- 1588 Jouan-Rimbaud D, Bouveresse E, Massart DL, de Noord OE (1999) Detection of prediction outliers
1589 and inliers in multivariate calibration. *Anal Chim Acta* 388:283–301
- 1590 Keller S, Löchte T, Dippel B, Schrader B (1993) Quality control of food with near-infrared excited
1591 Raman spectroscopy. *Fresenius J Anal Chem* 346:863–867
- 1592 Kennard RW, Stone LA (1969) Computer aided design of experiments. *Technometrics*
1593 11:137–148
- 1594 Kondepati VR, Heise HM (2008) The potential of mid- and near-infrared spectroscopy for reliable
1595 monitoring of bioprocesses. *Curr Trends Biotechnol Pharm* 2:117–132
- 1596 Kuligowski J, Quintás G, de la Guardia M, Lendl B (2010) Analytical potential of mid-infrared
1597 detection in capillary electrophoresis and liquid chromatography: a review. *Anal Chim Acta*
1598 679:31–42
- 1599 Kyriakidis NB, Skarkalis P (2000) Fluorescence spectra measurement of olive oil and other vegetable
1600 oils. *J AOAC Int* 83:1435–1438
- 1601 Lai YW, Kemsley EK, Wilson RH (1994) Potential of Fourier transform infrared spectroscopy for
1602 the authentication of vegetable oils. *J Agric Food Chem* 42:1154–1159
- 1603 Lakowicz JR (1999a) Principles of fluorescence spectroscopy, 2nd edn. Kluwer Academic
1604 Publishers, New York, pp 27–62
- 1605 Lakowicz JR (1999b) Instrumentation for fluorescence spectroscopy. In: Principles of fluorescence
1606 spectroscopy, 2nd edn. Kluwer Academic Publishers, New York, pp 25–60
- 1607 Lanser AC, Emken EA (1988) Comparison of FTIR and capillary gas chromatographic methods
1608 for quantitation of trans unsaturation in fatty acid methyl esters. *J Am Oil Chem Soc*
1609 65:1483–1487
- 1610 Lanser AC, List GR, Holloway RK, Mounts TL (1991) FTIR estimation of free fatty acid content
1611 in crude oils extracted from damaged soybeans. *J Am Oil Chem Soc* 68:448–449
- 1612 Levin IW, Lewis EN (1990) Fourier transform Raman spectroscopy of biological materials. *Anal*
1613 *Chem* 62:1101A–1111A
- 1614 Lewis EN, Kalasinsky VF, Levin IW (1988) Near-infrared Fourier transform Raman spectroscopy
1615 using fiber-optic assemblies. *Anal Chem* 60:2658–2661
- 1616 Li Y, García-González DL, Yu X, van de Voort FR (2008) Determination of free fatty acids in
1617 edible oils with the use of a variable filter array IR spectrometer. *J Am Oil Chem Soc*
1618 85:599–604
- 1619 Li D, Sedman J, García-González DL, van De Voort FR (2009) Automated acid content determination
1620 in lubricants by FTIR spectroscopy as an alternative to acid number determination.
1621 *J ASTM Int* 6:1–12
- 1622 Li-Chan ECY (1994) Developments in the detection of adulteration of olive oil. *Trends Food Sci*
1623 *Technol* 5:3–11
- 1624 Li-Chan ECY (1996) The application of Raman spectroscopy in food science. *Trends Food Sci*
1625 *Technol* 7:361–370
- 1626 Li-Chan ECY, Griffiths PR, Chalmers JM (2010a) Applications of vibrational spectroscopy in food
1627 science. Volume I: instrumentation and fundamental applications. Wiley, Chichester
- 1628 Li-Chan ECY, Griffiths PR, Chalmers JM (2010b) Applications of vibrational spectroscopy in
1629 food science. Volume II: analysis of food, drink and related material. Wiley, Chichester
- 1630 Ma K, van de Voort FR, Ismail AA, Sedman J (1998) Quantitative determination of hydroperoxides
1631 by FTIR spectroscopy using a disposable IR card. *J Am Oil Chem Soc* 75:1095–1101
- 1632 Ma K, van de Voort FR, Sedman J, Ismail AA (1999) *Trans* determination in fats and oils and
1633 margarine by FTIR spectroscopy using a disposable IR card. *J Am Oil Chem Soc*
1634 76:1399–1404
- 1635 Martens H, Naes T (1989) Multivariate calibration. Wiley, Chichester
- 1636 Massart DL, Kaufman L (1983) The interpretation of analytical chemical data by the use of cluster
1637 analysis. Wiley Interscience, Chichester
- 1638 Mossoba MM, Yurawecz MP, McDonald RE (1996) Rapid determination of the total *trans* content
1639 of neat hydrogenated oils by attenuated total reflection spectroscopy. *J Am Oil Chem Soc*
1640 73:1003–1009

- Muniategui S, Paseiro P, Simal J (1992) Medida del grado de insaturación de aceites y grasas comestibles por espectroscopia infrarroja y su relación con el índice de yodo. *Grasas Aceites* 43:1–5 1641–1643
- Naes T, Isaksson T (1989) Selection of samples for calibration in near-infrared spectroscopy. Part I: general principles illustrated by example. *Appl Spectrosc* 43:328–335 1644–1645
- Nicoletti GM (1990) La fluorescenza degli oli di oliva. *Riv Ital Sost Grasse* 67:389–396 1646
- O'Neill R (1971) Function minimization using a simplex procedure. *Appl Stat-J Roy St* 3:79–88 1647
- Osborne BG, Fearn T, Hindle PH (1993) Spectroscopy with application in food and beverage analysis. Longman Sci & Tech, Singapore, pp 1–77 and pp 120–141 1648–1649
- Ozaki Y, Cho R, Ikegaya K, Muraishi S, Kawachi K (1992) Potential of near-infrared Fourier transform Raman spectroscopy in food analysis. *Appl Spectrosc* 46:1503–1507 1650–1651
- Panford JA, Deman JM (1990) Determination of oil content of seeds by NIR: influence of fatty acid composition on wavelength selection. *J Am Oil Chem Soc* 67:473–482 1652–1653
- Patra D, Mishra AK (2002) Recent developments in multi-component synchronous fluorescence scan analysis. *Trac-Trends Anal Chem* 21:787–798 1654–1655
- Pell RJ (2000) Multiple outlier detection for multivariate calibration using robust statistical techniques. *Chemometr Intell Lab* 52:87–104 1656–1657
- Pfaffenberger RC, Dielman TE (1990) A comparison of regression estimators when both multicollinearity and outliers are present. In: Lawrence KD, Arthur JL (eds) *Robust regression: analysis and applications*. Marcel Dekker, New York, pp 243–270 1658–1659
- Poulli KI, Chantzos NV, Mousdis GA, Georgiou CA (2009a) Synchronous fluorescence spectroscopy: tool for monitoring thermally stressed edible oils. *J Agric Food Chem* 57:8194–8201 1660–1661
- Poulli KI, Mousdis GA, Georgiou CA (2009b) Monitoring olive oil oxidation under thermal and UV stress through synchronous fluorescence spectroscopy and classical assays. *Food Chem* 117:499–503 1662–1663
- Rabiner LR, Gold B (1975) *Theory and application of digital signal processing*. Prentice-Hall, Englewood Cliffs 1664–1665
- Ratnayake WMN, Pelletier G (1996) Methyl esters from a partially hydrogenated vegetable oil is a better infrared external standard than methyl elaidate for the measurement of total trans content. *J Am Oil Chem Soc* 73:1165–1169 1666–1667
- Sadeghi-Jorabchi H, Hendra PJ, Wilson RH, Belton PS (1990) Determination of the total unsaturation in oils and margarines by Fourier transform Raman spectroscopy. *J Am Oil Chem Soc* 67:483–486 1670–1671
- Sadeghi-Jorabchi H, Wilson RH, Belton PS, Edwards-Webb JD, Coxon DT (1991) Quantitative analysis of oils and fats by Fourier transform Raman spectroscopy. *Spectrochim Acta A* 47:1449–1458 1672–1673
- Sato T (1994) Near-infrared spectroscopic analysis of deterioration indices of soybeans for process control in *oil* milling plant. *J Am Oil Chem Soc* 71:293–298 1674–1675
- Sato T, Kawano S, Iwamoto M (1991) Near-infrared spectral patterns of fatty acid analysis from fats and oils. *J Am Oil Chem Soc* 68:827–833 1676–1677
- Savitsky A, Golay MJE (1964) Smoothing and differentiation of data by simplified least square procedures. *Anal Chem* 36:1627–1630 1678–1679
- Sayago A, García-González DL, Morales MT, Aparicio R (2007) Detection of the presence of refined hazelnut oil in refined olive oil by fluorescence spectroscopy. *J Agric Food Chem* 55:2068–2071 1680–1681
- Schrader B (1996) Raman spectroscopy in the near-infrared – a most capable method of vibrational spectroscopy. *Fresenius J Anal Chem* 355:233–239 1682–1683
- Scotter CNG (1997) Non-destructive spectroscopic techniques for the measurement of food quality. *Trends Food Sci Technol* 8:285–292 1684–1685
- Sharma A, Schulman SG (1999) Measurement of fluorescence spectra. In: *Introduction to fluorescence spectroscopy*. Wiley, New York, pp 69–99 1686–1687
- Sikorska E, Romaniuk A, Khmelinskii IV, Herance R, Bourdelande JL, Sokorski M, Koziol J (2004) Characterization of edible oils using total luminescence spectroscopy. *J Fluoresc* 14:25–35 1688–1693

- 1695 Sikorska E, Górecki T, Khmelinskii IV, Sokorski M, Koziol J (2005) Classification of edible oils
1696 using synchronous scanning fluorescence spectroscopy. *Food Chem* 89:217–225
- 1697 Sikorska E, Khmelinskii IV, Sikorski M, Caponio F, Bilancia MT, Pasqualone A, Gomes T (2008)
1698 Fluorescence spectroscopy in monitoring of extra virgin olive oil during storage. *Int J Food Sci*
1699 *Technol* 43:52–61
- 1700 Sinclair RG, McKay AF, Myers GS, Jones RN (1952) The infrared absorption spectra of saturated
1701 fatty acids and esters. *J Am Oil Chem Soc* 74:2578–2585
- 1702 Skoog DA, West DM, Holler FJ (1992) Fundamentals of analytical chemistry. Saunders College
1703 Publ Int Edition, New York
- 1704 Sleeter RT, Matlock MG (1989) Automated quantitative analysis of isolated (nonconjugated) *trans*
1705 isomers using Fourier transform infrared spectroscopy incorporating improvements in the pro-
1706 cedure. *J Am Oil Chem Soc* 66:121–127
- 1707 Snee RD (1977) Validation of regression models, methods and examples. *Technometrics*
1708 19:415–428
- 1709 Socrates G (1994) Infrared characteristic group frequencies: tables and charts. Wiley, New York
- 1710 Stefanov I, Baeten V, Abbas O, Colman E, Vlaeminck B, De Baets B, Fievez V (2010) Analysis of
1711 milk odd- and branched-chain fatty acids using Fourier transform (FT)-Raman spectroscopy.
1712 *J Agric Food Chem* 58:10804–10811
- 1713 Strasburg GM, Ludescher RD (1995) Theory and applications of fluorescence spectroscopy in
1714 food research. *Trends Food Sci Technol* 6:69–75
- 1715 Tabachnick BG, Fidell LS (1983) Using multivariate statistics. Harper & Row, New York
- 1716 Tai C, Gu X, Zou H, Guo Q (2002) A new simple and sensitive fluorometric method for the deter-
1717 mination of hydroxyl radical and its application. *Talanta* 58:661–667
- 1718 Tena N, García-González DL, Aparicio R (2009) Evaluation of virgin olive oil thermal deteriora-
1719 tion by fluorescence spectroscopy. *J Agric Food Chem* 57:10505–10511
- 1720 Tena N, Aparicio R, García-González DL (2012) Chemical changes of thermoxidized virgin olive
1721 oil determined by excitation-emission fluorescence spectroscopy (EEFS). *Food Res Int*
1722 45:103–108
- 1723 Ulberth F, Haider HJ (1992) Determination of low level *trans* unsaturation in fats by Fourier trans-
1724 form infrared spectroscopy. *J Food Sci* 57:1444–1447
- 1725 Valeur B (2002) Molecular fluorescence: principles and applications. Wiley-VCH Verlag,
1726 Weinheim
- 1727 van de Voort FR (1994) FTIR spectroscopy in edible oil analysis. *Inform* 5:1038–1042
- 1728 van de Voort FR, Ismail AA (1991) Proximate analysis of foods by mid-FTIR spectroscopy. *Trends*
1729 *Food Sci Technol* 2:13–17
- 1730 van de Voort FR, Sedman J, Emo G, Ismail AA (1992) Rapid and direct iodine value and saponifi-
1731 cation number determination of fats and oils by attenuated total reflectance/fourier transform
1732 infrared spectroscopy. *J Am Oil Chem Soc* 69:1118–1123
- 1733 van de Voort FR, Ismail AA, Sedman J, Dubois J, Nicodemo T (1994a) The determination of per-
1734 oxide value by Fourier transform infrared spectroscopy. *J Am Oil Chem Soc* 71:921–926
- 1735 van de Voort FR, Ismail AA, Sedman J, Emo G (1994b) Monitoring the oxidation of edible oils by
1736 Fourier transform infrared spectroscopy. *J Am Oil Chem Soc* 71:243–253
- 1737 van de Voort FR, Ismail AA, Sedman J (1995) A rapid automated method for the determination of
1738 cis and trans content of fats and oils by Fourier transform infrared spectroscopy. *J Am Oil*
1739 *Chem Soc* 72:873–880
- 1740 van de Voort FR, Memon KP, Sedman J, Ismail AA (1996) Determination of solid fat index by
1741 FTIR spectroscopy. *J Am Oil Chem Soc* 73:411–416
- 1742 van de Voort FR, Cocciardi R, Sedman J, Juneau S (2007a) An automated FTIR method for the
1743 routine quantitative determination of moisture in lubricants. *Talanta* 72:289–295
- 1744 van de Voort FR, Sedman J, Sherazi STH (2007b) Improved FTIR trans analysis in edible oils
1745 using spectral reconstitution. *J AOAC Int* 90:446–451
- 1746 van de Voort F, Ghetler A, García-González DL, Li Y (2008) Perspectives on quantitative Mid-
1747 FTIR spectroscopy in relation to edible oil and lubricant analysis: evolution and integration of
1748 analytical methodologies. *Food Anal Method* 1:153–163

Vapnik VN (2000) The nature of statistical learning theory, 2nd edn. Springer, New York	1749
Vonach R, Lendl B, Kellner R (1997) Hyphenation of ion exchange high-performance liquid chromatography with Fourier transform infrared detection for the determination of sugars in nonalcoholic beverages. <i>Anal Chem</i> 69:4286–4290	1750 1751 1752
Wetzel DL (1983) Lipid structures and NIRA. In: Proceedings of 4th international symposium NIRA, Manhattan	1753 1754
Williams PC, Antoniszyn J (1987) The significance of outliers. In: Proceedings of international NIR/NIT conference, Kiadó Akadémiai, Budapest. pp 249–264	1755 1756
Williams P, Norris K (2001) Near-infrared technology in the agricultural and food industries, 2nd edn. American Association of Cereals Chemists, St Paul	1757 1758
Wilson RH (1990) Fourier transform mid-infrared spectroscopy for food analysis. <i>Trends Anal Chem</i> 9:127–131	1759 1760
Wilson RH, Goodfellow BJ (1994) Mid-infrared spectroscopy. In: Wilson RH (ed) Spectroscopic techniques for food analysis. Verlagsgesellschaft (VCH), New York, pp 59–85	1761 1762
Wilson EB, Decius JC, Cross PC (1955) Molecular vibrations: the theory of infrared and Raman vibrational spectra. McGraw-Hill, New York	1763 1764
Wolfbeis OS, Leiner M (1984) Charakterisierung von speiseölen mit hilfe der fluoreszenztopographie. <i>Mikrochim Acta</i> 1:221–233	1765 1766
Yu X, Du S, van de Voort FR, Yue T, Li Z (2009) Automated and simultaneous determination of free fatty acids and peroxide values in edible oils by FTIR spectroscopy using spectral reconstruction. <i>Anal Sci</i> 25:627–632	1767 1768 1769
Zandomeneghi M, Carbonaro L, Caffarata C (2005) Fluorescence of vegetable oils: olive oils. <i>J Agric Food Chem</i> 53:759–766	1770 1771

Author Queries

Chapter No.: 10 0001997388

Queries	Details Required	Author's Response
AU1	Do you mean more sophisticated? Generally, sophistication is good when it comes to tools. Perhaps you mean less complicated?	
AU2	Inserted "adopted" here as there was no verb for this item. Please confirm.	
AU3	Inserted "Fourier transform infrared spectroscopy" before "FTIR" since it hasn't been defined yet. Please confirm.	
AU4	In the title for Table 10.2, this is hyphenated: FT-IR. Please decide how you'd like to write it and impose consistency globally.	
AU5	Changed the outer parentheses to square brackets to avoid nested parentheses). Please confirm.	
AU6	Changed "in" to "on" before "all electrons" (usually you say "exert a force on something else"). Please confirm.	
AU7	Please specify "a" or "b" of Patra and Mishra (2002).	
AU8	Changed "appropriated" to "appropriate" and "according to" to "based on." Please confirm.	
AU9	Please specify "a" or "b" of Lakowicz (1999).	
AU10	The original had "in the case of oils 1% it is enough." Please confirm changes.	
AU11	The original had "One of the main reasons," but it seems that two are given. Please confirm.	
AU12	Please provide details of Osborne et al. (1997), Sharma et al. (1999), Cayuela et al. (2010), Defernez et al. (1996), Williams and Norris (1987), Sadeghi-Jorabchi (1991) in the reference list.	
AU13	Inserted "to" here. Please confirm.	
AU14	The list of abbreviations at the beginning of the chapter gives "reflection" as the definition of "R" is "ATR." Please verify and change one of them.	
AU15	Moved the closing parenthesis from after "crystal" to after "ATR." Please confirm.	
AU16	Changed "right" to "correct" before "calibration." Please confirm.	
AU17	It is unclear what is meant by this. Do you mean "means there will be problems in sample handling" or "raises the issue of sample handling" or something else? Please revise.	
AU18	"Aspired" does not make sense here. Do you mean "aspirated"?	
AU19	In general, this is written without hyphenation, FTIR, but please decide how you'd like to write it and impose consistency.	

AU20	Change “informs” to “provides information.” Please confirm.	
AU21	Inserted “spectroscopy” here.	
AU22	Changed “NIRS” to “NIR spectroscopy.”	
AU23	Changed “assignation” to “assignment.”	
AU24	Please check if inserted citation for Figure 10.14 is okay.	
AU25	In “For a thorough presentation of the ideas in this section,” added “the ideas in.” Please confirm.	
AU26	Inserted “of the model” here.	
AU27	Italicized “N” here and below.	
AU28	Italicized “M” here and below.	
AU29	“PCR” was originally not defined. I inserted “polymerase chain reaction” before it. If it’s not used again, perhaps the abbreviation could be deleted?	
AU30	Originally, “(i = 0,1,...,>N)” was superscripted, but it was raised up to the normal line. Please confirm.	
AU31	This does not appear in the list of abbreviations. Should it?	
AU32	Inserted “spectroscopy” here. Please confirm.	
AU33	Changed “thermal” to “thermally” here. Please confirm.	
AU34	Duplicate references of Patra and Mishra has been deleted. Please check if okay.	
AU35	Please cite Cayuela and Pérez Camino (2010), Jiménez-Márquez et al. (2005), Sharma and Schulman (1999) in text.	